Calhoun: The NPS Institutional Archive

DSpace Repository

Theses and Dissertations | 1. Thesis and Dissertation Collection, all items

1992

Statistical fatigue analysis of the SH-60B servo beam rail component.

deGozzaldi, Sally

Monterey, California. Naval Postgraduate School

http://hdl.handle.net/10945/24044

NAVAL POSTGRADUATE SCHOOL
Monterey, California

THESIS

STATISTICAL FATIGUE ANALYSIS
OF THE
SH-60B SERVO BEAM RAIL COMPONENT

by

Sally deGozzaldi

September, 1992

Thesis Advisor: Gerald H. Lindsey

Approved for public release; distribution is unlimited

REPORT DOCUMENTATION PAGE

1a. REPORT SECURITY CLASSIFICATION UNCLASSIFIED	1b. RESTRICTIVE MARKINGS
2a. SECURITY CLASSIFICATION AUTHORITY	3. DISTRIBUTION/AVAILABILITY OF REPORT Approved for public release; distribution is unlimited.
2b. DECLASSIFICATION/DOWNGRADING SCHEDULE	

4. PERFORMING ORGANIZATION REPORT NUMBER(S)	5. MONITORING ORGANIZATION REPORT NUMBER(S)

6a. NAME OF PERFORMING ORGANIZATION Naval Postgraduate School	6b. OFFICE SYMBOL *(If applicable)* 31	7a. NAME OF MONITORING ORGANIZATION Naval Postgraduate School
6c. ADDRESS *(City, State, and ZIP Code)* Monterey, CA 93943-5000		7b. ADDRESS *(City, State, and ZIP Code)* Monterey, CA 93943-5000

8a. NAME OF FUNDING/SPONSORING ORGANIZATION	8b. OFFICE SYMBOL *(If applicable)*	9. PROCUREMENT INSTRUMENT IDENTIFICATION NUMBER

8c. ADDRESS *(City, State, and ZIP Code)*	10. SOURCE OF FUNDING NUMBERS			
	Program Element No.	Project No.	Task No.	Work Unit Accession Number

11. TITLE *(Include Security Classification)*

STATISTICAL FATIGUE ANALYSIS OF THE SH-60B SERVO BEAM RAIL COMPONENT

12. PERSONAL AUTHOR(S) deGozzaldi, Sally NMN

13a. TYPE OF REPORT Master's Thesis	13b. TIME COVERED From To	14. DATE OF REPORT *(year, month, day)* September, 1992	15. PAGE COUNT 86

16. SUPPLEMENTARY NOTATION

The views expressed in this thesis are those of the author and do not reflect the official policy or position of the Department of Defense or the U.S. Government.

17. COSATI CODES			18. SUBJECT TERMS *(continue on reverse if necessary and identify by block number)*
FIELD	GROUP	SUBGROUP	Fatigue Analysis, SH-60B, Weibull Distribution Analysis, Extreme Value Distribution Analysis, Servo Beam Rail

19. ABSTRACT *(continue on reverse if necessary and identify by block number)*

Statistical methods were researched to better understand the effect of the flight loads on the servo beam rail component of the SH-60B helicopter. The extreme value distribution and the Weibull distribution were used to model the distribution of flight loads. Specifically, the flight loads for the symmetric pullout maneuver were studied. Both models successfully represented the data, although more data are required to be fully confident in these representations. Different flight characteristics indicate that various factors such as gross weight, airspeed, and collective position effect the distribution of loads. The model runs indicate a good representation of the individual runs in fatigue life calculations. The damage calculated for the Sikorsky substantiation load run was less conservative than the model run. In addition, the maximum load of the substantiation run was only in the 45th percentile of the load distribution estimated using an extreme value distribution for loads. The damage calculated for the Sikorsky substantiation load run was more conservative than the damage calculated for the individual runs which was reduced as much as 100 times when corrected for mean load.

20. DISTRIBUTION/AVAILABILITY OF ABSTRACT			21. ABSTRACT SECURITY CLASSIFICATION UNCLASSIFIED	
☒ UNCLASSIFIED/UNLIMITED	☐ SAME AS REPORT	☐ DTIC USERS		
22a. NAME OF RESPONSIBLE INDIVIDUAL Gerald H.. Linsey		22b. TELEPHONE *(Include Area code)* (408) 646-2808		22c. OFFICE SYMBOL AA/LI

DD FORM 1473, 84 MAR   83 APR edition may be used until exhausted   SECURITY CLASSIFICATION OF THIS PAGE
All other editions are obsolete   UNCLASSIFIED

Statistical Fatigue Analysis of the SH-60B
Servo Beam Rail Component

by

Sally deGozzaldi
Lieutenant, United States Navy
B.A., Amherst College

Submitted in partial fulfillment
of the requirements for the degree of

MASTER OF SCIENCE IN AERONAUTICAL ENGINEERING

from the

NAVAL POSTGRADUATE SCHOOL
September, 1992

ABSTRACT

Statistical methods were researched to better understand the effect of flight loads on the servo beam rail component of the SH-60B helicopter. The extreme value distribution and the Weibull distribution were used to model the distribution of flight loads. Specifically, the flight loads for the symmetric pullout maneuver were studied. Both models successfully represented the data, although more data are required to be fully confident in these representations. Different flight characteristics indicate that various factors such as gross weight, airspeed, and collective position effect the distribution of loads. The model runs indicate a good representation of the individual runs in fatigue life calculations. The damage calculated for the Sikorsky substantiation load run was less conservative than the model run. In addition, the maximum load of the substantiation run was only in the 45th percentile of the load distribution estimated using an extreme value distribution for loads. The damage calculated for the Sikorsky substantiation load run was more conservative than the damage calculated for the individual runs which was reduced as much as 100 times when corrected for mean load.

CONTENTS

I. INTRODUCTION

A. PURPOSE AND OBJECTIVE

The general purpose of this thesis was to more accurately determine the fatigue life of critical helicopter components. Currently methods of fatigue analysis for such components are a topic of research [Ref.'s 1,2,3,4,5,6,7]. The specific objective was to create a statistical load model for the symmetrical pullout maneuver and to compare the resulting fatigue life predictions of a critical component with the fatigue life determined using loads obtained from flight test substantiation runs.

The SH-60B was the helicopter studied. It is a single main rotor, twin-engine helicopter manufactured by the United Technologies Corporation, Sikorsky Aircraft Division. It is configured specifically in response to the Light Airborne Multipurpose System (LAMPS) requirement of the U.S. NAVY. The primary mission is Anti-Submarine Warfare (ASW). The major secondary mission is Anti-ship Surveillance and Targeting (ASST). Its threat encompasses a hostile submarine fleet and missile-equipped surface ships. This system extends the search and attack capabilities of the LAMPS MK III configured destroyer, frigate, and cruiser platforms [Ref. 8].

B. BACKGROUND

The safe-life approach is the fatigue analysis method adopted by the Navy. Historically, this approach involved

1

assigning   component retirement times by flight hours.
Component flight hour logs were maintained, and once the
assigned component reached a certain flight time, the
component was retired. In order to determine the component's
retirement time, a study of each component's fatigue life was
completed.

1. Fatigue Life

To determine the fatigue life, the component's
maneuver spectrum, which includes the mix of maneuvers
experienced, the variable loads for each maneuver, the
material fatigue behavior, and the resulting fatigue damage
were all evaluated.

a. Maneuver Spectrum

The maneuver spectrum is the percentage of time
assumed for different flight conditions during the mission of
the helicopter.   It includes all the critical maneuvers
anticipated for the helicopter in 100 flight hours while it
flies its intended mission.

b. Flight Load Spectrum

Flight load variability is experienced for each
maneuver and is measured by flying the same model rotor-craft
under the same conditions and in accordance with a usage
spectrum while recording the variations in the flight loads
[ref 3]. The variation in flight loads for a given maneuver
is called the flight load spectrum.

c. **Component Stress Life (S-N) Curve**

Typically, component stress life is determined by bench testing six full scale component test specimens under constant amplitude loading at various levels. The endurance limit of each full scale specimen is determined by matching its failure point, to an appropriate material S-N curve. The arithmetic mean of the six endurance limits is used. The endurance limit is then reduced to represent a true mean minus three standard deviations. This reduction in the endurance limit is generated by one of three methods: subtracting three times the standard deviation, taking eighty percent of the mean, or taking the lowest strength specimen in the sample. In addition, the mean S-N curve is further reduced by the constant coefficient of variation reduction. This is the ratio of the reduced mean to the mean endurance limit. [Ref. 2] The end product is the component S-N curve.

d. **Damage Calculation**

Damage calculations are based on Miner's rule of linear cumulative damage indicated by the following equation (1):

$$D = \sum \frac{n_i}{N_i} \qquad (1)$$

When D=1, fatigue failure is predicted to occur. The n_i is the anticipated number of cycles at a given load and N_i is the allowable cycles at the same load level as defined by the S-N curve.

e. Comments about the Method

The determination of a safe replacement time depends on introducing at least six weaknesses in the analysis, which effects the conservatism of the analysis. First, the flight spectrum considered does not include operational variability. If the load severity of the flight test aircraft is high relative to the fleet aircraft, the conservatism would increase and the reliability would improve. Conversely, if the load severity of the flight test aircraft is lower than the fleet, the lighter spectrum would decrease the conservatism and adversely affect the component reliability [Ref. 2].

The second weakness is the use of the working S-N curve, the usage spectra, and the top flight test data loads [Ref. 1]. This unknown adds conservatism which could result in a part mean life decreasing from 200,000 hours to 5000 hours [Ref. 1]. The third weakness is that the component strength represented by the component S-N curve did not factor in life variability due to manufacture techniques, manufacture anomalies, mishandling, or environmental conditions [Ref. 3].

4

The fourth weakness is that the small size of the bench test samples leads to reduced confidence in estimating all the failure mechanisms. Additional failure mechanisms could decrease the conservatism and have an adverse affect on reliability [Ref. 2]. The fifth weakness is the collection of conservative assumptions made to reduce the complexity of damage calculations and to limit the scope of flight test data requirements. The sixth weakness is that the highest load level observed within the available applicable pool is the basis for the damage calculation [Ref. 4]. These six weaknesses effect the overall reliability of the safe life method. Statistical methods are being researched in an attempt to evaluate some of these weaknesses.

2. History of Statistical Approach

Previous studies have attempted to increase the reliability of the safe life approach. Statistical processes have been adopted in order to more accurately depict the fatigue life of a component and thus to substantiate the safe life approach. Safe life reliability is the conditional probability, at a given confidence level, that a dynamic component will meet, or exceed, the prescribed safe life under a presumed set of operating conditions [Ref. 2]. Analytical procedures were used in these studies to assess the probability that a given rotor-craft component would not fail in service due to fatigue. As many factors as possible were

looked at in order to confidently estimate component reliability. These procedures consider variations in strength of the components due to standard manufacture, manufacturing anomalies, mishandling, environmental degradation etc., variations in flight loads, and variations in the usage rate of the rotor-craft. [Ref. 3] Three factors; maneuver spectrum, component fatigue strength, and flight load variability were determined to have the greatest impact on reliability [Ref. 2]. The confidence in the reliability of the safe life approach depends on the degree of certainty to which the estimated distribution of these dominant factors actually represent their true distributions [Ref. 2].

a. Maneuver Spectrum

Aircraft usage involves determining the mission segments, flight conditions, percent usage, and a brief description of the type of flying. This factor was not researched in this study. The mission segment, flight conditions, percent usage, type of flying have been determined previously.

b. Component Stress Life (S-N) Curve

Computational component fatigue stress, as determined by the safe life fatigue method, incorporates many assumptions. One area which has been studied is the method of reducing the mean curve in the low cycle fatigue region. Two methods are used to reduce the S-N curve; the constant

6

coefficient of variation (CCV) and the constant standard deviation (CSD). The CCV method is considered more conservative. [Ref. 2] Comparison of these two statistical methods was not completed in this study. The CCV method was used.

c. Flight Load Distribution

Flight load distribution has been studied previously along the following lines. First, the expected flight loads were estimated by the cumulative histogram of load cycles from all candidate flight events. All loads occurring within a particular load range were conservatively placed at the upper band edge of the range. The histogram was analyzed using the two parameter Weibull distribution. The validity of this method has been checked and good results were found when comparing the resulting safe life reliability, using the predicted data, to the resulting safe life reliability, using the actual data. The reliability was also evaluated by comparing the lives calculated, as a function of endurance limit, using the top load criteria, to the lives calculated, as a function of endurance limit, using the expected loads. The reliability was obtained by calculating the number of sample standard deviations of strength reduction, from the sample mean, and extracting the cumulative probability from a standard normal distribution. The conclusions found from these previous studies were that the

loads calculated statistically refine the implicit reliability over the discrete loads obtained from the histogram, with its conservative upward biasing. The extent of the benefit seems to depend on the distribution of load and the component S/N curve shape. [Ref. 2]

The following thesis will reproduce many of the methods previously researched in order to better understand the statistical distributions used in predicting flight load populations. The fatigue life of the statistically determined load spectrum will be compared to fatigue life of the raw data load spectrum. In Chapter II the flight test data is described, in Chapter III statistical treatment of the data is discussed, in Chapter IV a fatigue analysis of the data is completed and in Chapter V a summary and the conclusions are provided.

II. FLIGHT TEST DATA

A. DESCRIPTION OF SUBSTANTIATION FLIGHT TESTS

United Technologies Corporation, Sikorsky Aircraft Division, conducted substantiation flight tests to determine the fatigue life of certain fatigue critical components. Four to five substantiation runs were typically made for each maneuver. The run with the highest maximum load was used to substantiate the fatigue life. Figure 1 depicts the substantiation test data used by Sikorsky for the symmetric pullout maneuver. The 'plot 2.0' data indicates symmetric pullout runs which produced accelerations over two g's. The airspeed was 155 knots and the gross weight was between 19,000 and 21,000 lbs. The 'loadlev' column indicates the load magnitude for the maneuver. The 'occur' column is the number of occurrences of this particular symmetric pullout maneuver in 100 hours. The 'cyc' column is the number of times the load level was experienced during the maneuver. The 'allowcyc' is the number of cycles at that level that would produce failure as determined from the component S-N curve, and the 'dam' column is the calculated fatigue damage. The maneuver spectrum was also provided by Sikorsky. See Table 1 for a sample SH-60B maneuver spectrum.

```
*****CYCLE COUNT 5*****

                    LOADLEV   OCCUR   CYC   ALLOWCYC      DAM
    ****  ********  *******   *****   ***   ********   **********
     44   PLOT 2.0    4490      20      3       1.01      .0001
                      3880              6       2.99      .0000
                      3290              9      32.30      .0000
                      2700              7    INF.         .0000
                      2110              5    INF.         .0000


    TOTAL DAMAGE THIS MANEUVER = .0001
```

Figure 1: Sikorsky Substantiation Run Data

TABLE 1: MANEUVER SPECTRUM

SIKORSKY AIRCRAFT

SH-60B FATIGUE DAMAGE CALCULATION
TABLE A-1

SER-520103
Revision 1 - 5/15/80
Revision 2 - 11/14/80

COMPONENT: _____
P/N: _____
FRACTURE MODE: _____
LOADING FREQUENCY: _____ CPS

SUBSTANTIATING PARAMETER: _____
CURVE SHAPE: _____
WORKING ENDURANCE LIMIT (@ 10^8): _____
VIRTUAL ENDURANCE LIMIT: _____
(For Comparison Purposes Only)

G.W RANGE: 14 500 LB TO 21,700 LB
C.G. RANGE 342.6 TO 363.0
ROTOR SPEED 96% TO 100.5% NR

NO	REGIME	TV MAX	θ TIME	MAN PER 100 HOURS	SECS PER MAN	FLIGHT LOAD	FLIGHT AND MAN NO.	ALLOW CYCLES 10^	DAMAGE PER 100 HOURS	NO	REGIME	TV MAX	θ TIME	MAN PER 100 HOURS	SECS PER MAN	FLIGHT LOAD	FLIGHT AND MAN NO.	ALLOW CYCLES 10^	DAMAGE PER 100 HOURS
1	CONTROL CHECKS	0		100						37	45° A.O.G. RIGHT TURN	90	.25	90	10				
2	ROTOR & PYLON SPREAD		70							38	LONG. REV. HOVER	0		330	1.0				
3	ROTOR & PYLON FOLD		70							39	LONG. REV. FWD. FLT.	100		270	1.0				
4	ROTOR ENGAGEMENT			100						40	LAT. REV. HOVER	0		330	1.0				
5	ROTOR SHUTDOWN			100						41	LAT. REV. FWD. FLT.	100		270	1.0				
6	TAXI, TAXI TURNS, BRAKING		7.0	400	10					42	YAW REV. HOVER	0		330	1.0				
7	HOVER		6.0							43	YAW REV. FWD. FLT.	100		270	1.0				
8	LEFT HOVER TURN	0	1.7	500	12					44	2.0g PULLOUT	100		20	2.0				
9	RIGHT HOVER TURN	0	1.7	500	12					45	1.5g PULLOUT	100		100	5.0				
10	LEFT SIDE FLIGHT		0.5	110	117					46	POWER DIVE	140	1.0	190	15				
11	RIGHT SIDE FLIGHT		0.5	110	117					47	AUTO. (ENTRY)	70		40	12.0				
12	REARWARD FLIGHT		0.5	110	117					48	STEADY AUTO.	70	1.0						
13		20% V MAX	70	5.0							49	AUTO. RECOVERY	70		40	12.0				
14		40% V MAX	40	7.0							50	AUTO. LEFT TURN	70	10.2	50	10				
15		50% V MAX	50	7.0							51	AUTO. RIGHT TURN	70	10.2	50	115				
16		60% V MAX	60	5.0							52	CONTROL REV. AUTO.	70		300	1.0				
17	LEVEL FLIGHT	70% V MAX	70	13.0							53	AUTO. PULLOUT	70		40	1.0				
18		80% V MAX	80	15.5							54	AUTO. APPROACH & LANDING	140	0.3	40	27.0				
19		90% V MAX	90	15.0							55	DROOP STOP POUNDING			1100	2.0				
20		100% V MAX	100	8.7							56	B.A.G. (W/ROTOR STOP)			1100					
21		110% V MAX	110	1.0							57	B.A.G. (W/O ROTOR STOP)			400					
22	PARTIAL POWER DESCENT	80	1.0	500	12					58									
23	LEFT SIDESLIP	100	0.5							59									
24	RIGHT SIDESLIP	100	0.5							60									
25	JUMP TAKE-OFF			150	7.0					61									
26	ROLLING TAKE-OFF (3000CAS)			40	7.0					62									
27	VERTICAL TAKE-OFF			200	7.0					63									
28	T.O. POWER CLIMB		1.0							64									
29	MAX. CONT. POWER CLIMB		1.0							65									
30	APPROACH	140	1.2	440	10.0					66									
31	LANDING FROM HOVER	0		140	5.0					67									
32	R.A.S.T. ARRESTMENT	0		140	7.0					68									
33	RUN-ON LANDING	20		40	7.0					69									
34	30° A.O.G. LEFT TURN	90-100	2.25	100	15					70									
35	30° A.O.G. RIGHT TURN	90-100	2.25	100	10					71									
36	45° A.O.G. LEFT TURN	90	.25	90	10														

SUBTOTAL 1

TOTAL DAMAGE PER 100 HRS: _____

CALCULATED CRACK INITIATION TIME: 100/ _____ = _____ HRS.

SUBTOTAL.

1. Description of Symmetric Pullout Maneuver

The symmetric pullout maneuver was begun at an airspeed slightly greater than the goal airspeed with no lateral or directional central input. It was initiated by a single longitudinal input provided by cyclic control. At the same time the collective, which simultaneously controls the angle of attack of all the blades, was set at a pre-determined position. The cyclic and collective control positions were then held fixed until the target airspeed and acceleration were met. The controls were then neutralized to return to straight and level flight at the pre-maneuver airspeed. Note that two airspeeds were used (124 knots and 155 knots), three collective settings (fixed collective, -25% collective, and top collective) and numerous max g loads were obtained (from 1.5 g's to 3.4 g's).

2. Concentration on Symmetric Pullout Maneuver

The Systems Engineering Division, Code 1260, David Taylor Research Lab, provided excerpts of flight test data, the majority of which was for the symmetric pullout maneuver. It consisted of the entire load histories of 14 symmetric pullout runs conducted at two different flight speeds, three collective settings, and numerous 'g' loads. Maximum load data were also provided for 78 runs of several different maneuvers. Thirty five of the maximum load data points were for symmetric pullouts for two different gross weights.

B. SOURCE AND FORM OF DATA RECEIVED FROM DAVID TAYLOR LAB

1. Load Time Curves

Load measurements were made on the main rotor forward longitudinal stationary star (MRFLSS) during the different maneuvers of the SH-60B helicopter. The MRFLSS puts a load on the servo beam rail, a fatigue critical component with a Sikorsky part number 70219-02134-048. The MRFLSS is part of the flight control servo which directly connects the mixing unit to the swashplate. The hydraulic servo tilts the swashplate assemble, which moves the control rods attached to each spindle, directly controlling the movement of the rotor blades. The star loads are the loads placed on the swashplate component which is directly attached to the servos. The measurements were sampled four times per rotor revolution. The load (lbs.) and the time (sec) was recorded. Figures 2a through 2j and Figures 3a through 3d depict the graphical representation of the load-time trace for all symmetric pullout runs. Each run was approximately 25 seconds long, and the maximum loads ranged from approximately 2000 to 6000 lbs.
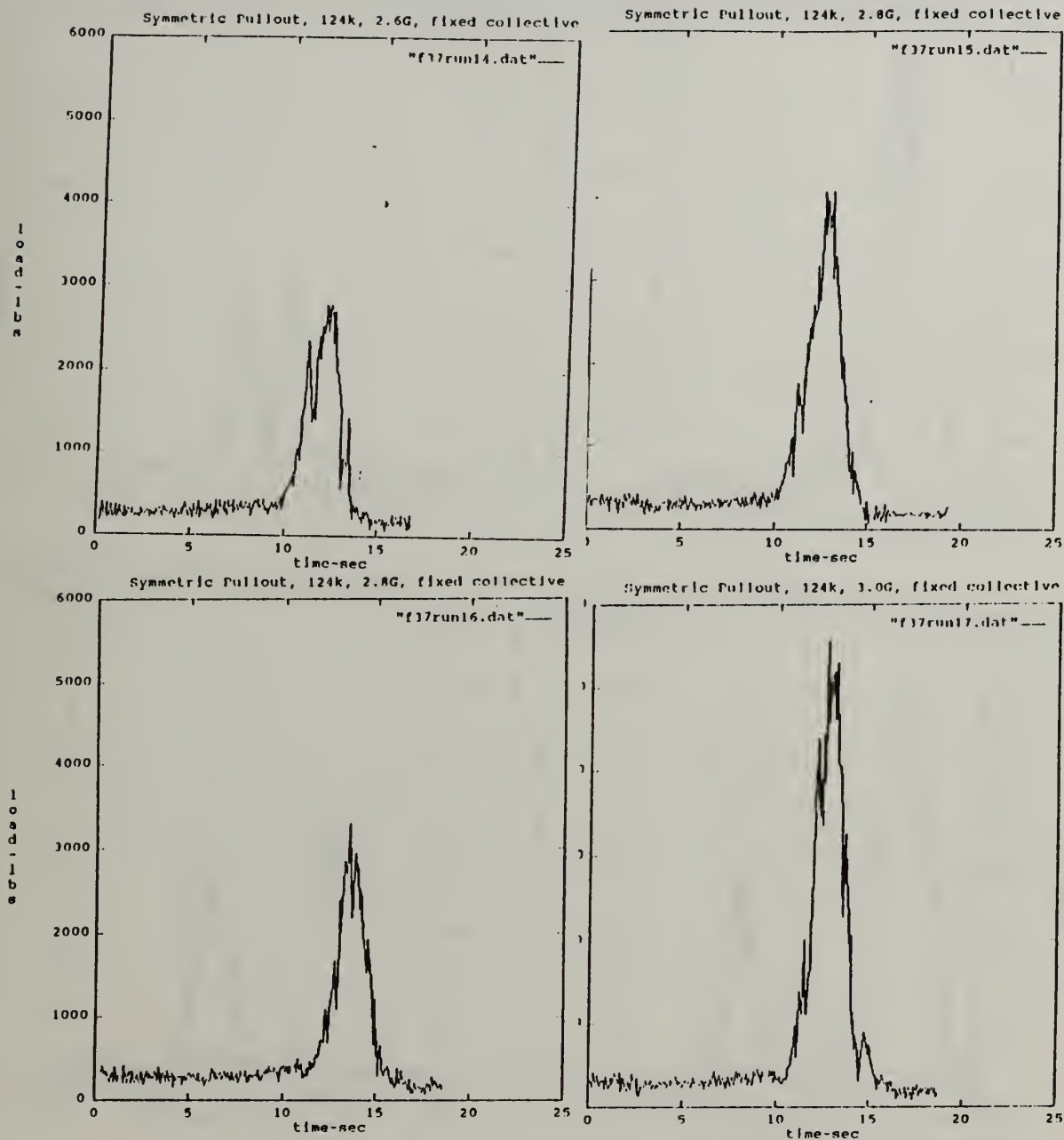
Figure 2a, 2b, 2c, and 2d:
Graphical Representation of Symmetric Pullout,
Runs 14, 15, 16, and 17

13
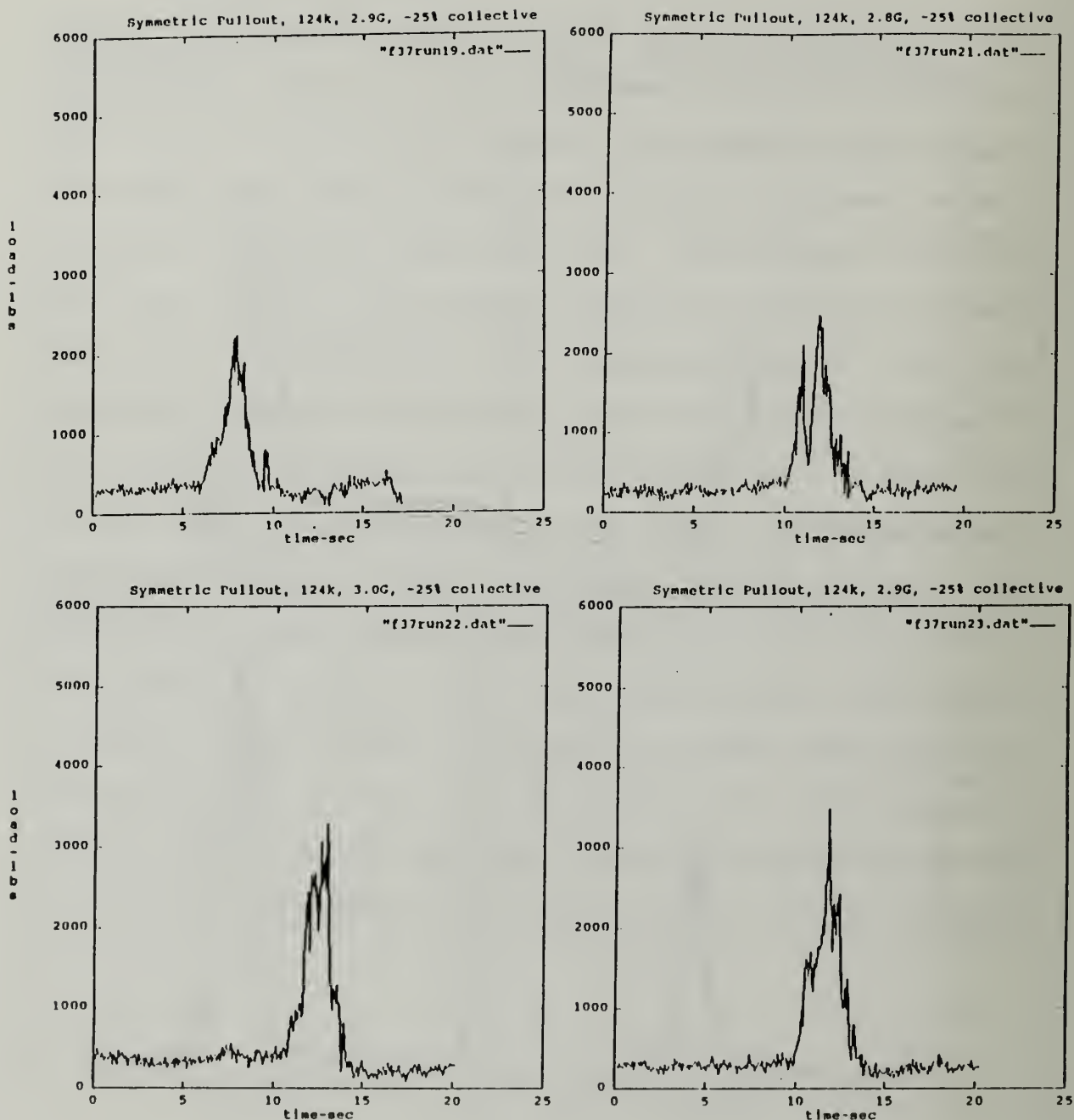
Figure 2e, 2f, 2g, and 2h:
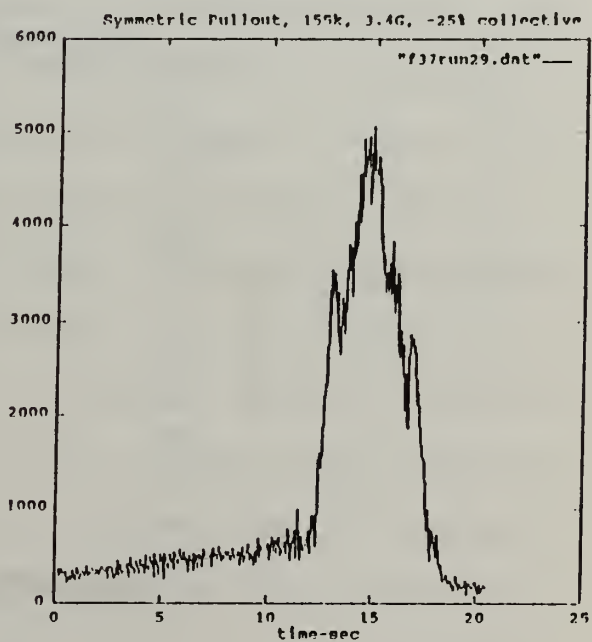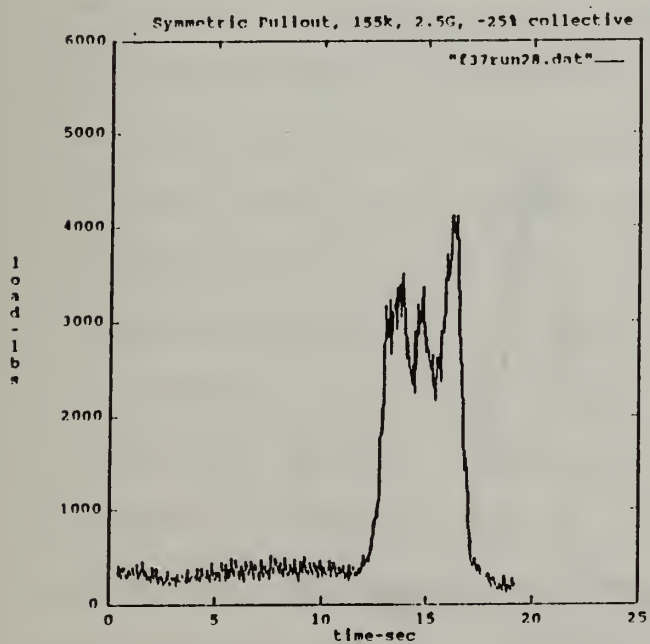Graphical Representation of Symmetric Pullout,
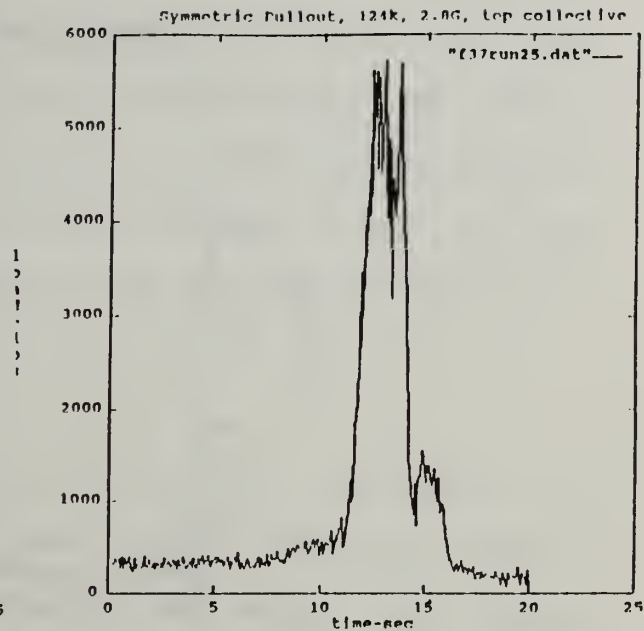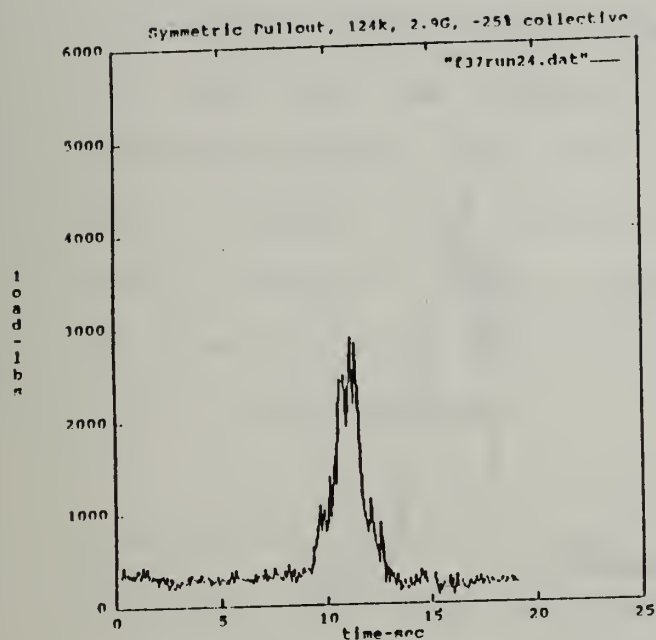Runs 19, 21, 22, and 23

14

Figure 2i, 2j, 3a, and 3b:
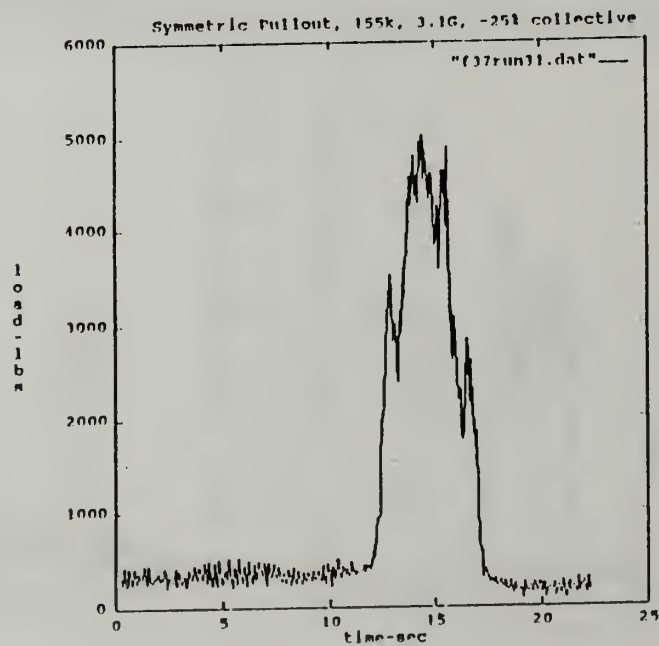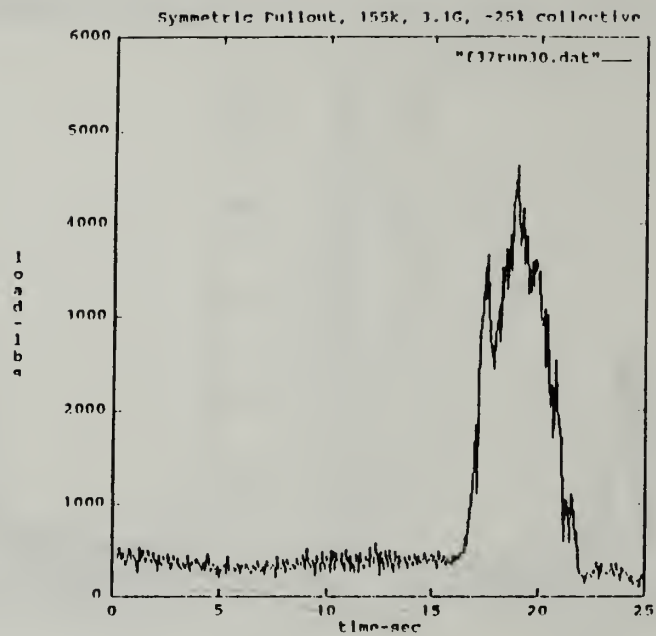Graphical Representation of Symmetric Pullout,
Runs 24, 25, 28, and 29:

15

Figure 3c and 3d:
Graphical Representation of Symmetric Pullout,
Runs 30 and 31

16

2. Maximum Load Data

Maximum load data were provided for 78 different runs encompassing 8 maneuvers. The majority of the maximum load data were for the symmetric pullout maneuver, but other maneuvers included: left turn, right turn, left climbing turn, right climbing turn, left rolling pullout, right rolling pullout, and dive. Table 2 contains the maximum load data for the symmetric pullout maneuver.

3. Major Variables

The velocity, collective position, maximum 'g' acceleration recorded, and gross weight were the major variables identified which affected the data. The gross weight for the 14 complete load histories was 16,500 lbs. Ten of the fourteen load histories were conducted at 124 knots. The remaining four were conducted at 155 knots. Five of the 124 knot runs were conducted with fixed collective. Six were conducted with -25 percent collective, and one was conducted with top collective. All the 155 knot runs were conducted at -25 percent collective. The 'g' loadings varied virtually with every flight. Because the 'g' loading runs were not repeated, interpretation of the 'g' loading affects was not attempted. The max load data provided data points from both the 16,500 lbs gross weight flight and from a 20,800 gross weight flight. Individual load-time histories from the 20,800 gross weight flight were not available.

17

TABLE 2: MAXIMUM LOAD DATA SUMMARY

SH-60 MAXIMUM LOAD DATA					
Flight 37: 16,500 gross wt.			Flight 43: 20,800 gross wt.		
RUN	MANEUVER	LOAD	RUN	MANEUVER	LOAD
19	SYM PULL (SP), 124K FIX COLL (FC), 2.6G	2783 LBS	69	SP, 124K, 100% TORGUE (100%), 1.5G	4262 LBS
16	SP, 124K, FC, 2.8G	4083	70	SP,124K,100%,1.75G	4513
16	SP, 124K, FC, 2.8G	3280	71	SP,124K,100%,2.0G	5652
17	SP, 124K, FC, 3.0G	5555	72	SP,124K,105%,2.0G	4466
16	SP, 124K, FC, 3.1G	5233	73	SP,124K,100%,2.1G	6993
19	SP, 124K, -25% COLL (-25%), 2.9G	2227	74	SP,124K,100%,2.1G	4646
20	SP, 124K,-25%, 2.7G	2237	75	SP,124K,100%,1.75G	4579
21	SP, 124K,-25%, 2.8G	2473	70	SP,124K,100%,2.1G	6055
22	SP, 124K,-25%, 3.0G	3276	77	SP,124K,100%,2.3G	6675
23	SP, 124K,-25%, 2.9G	3472	81	SP,155K,100%,1.5G	6701
24	SP, 124K,-25%, 2.9G	2873	82	SP,155K,100%,1.75G	6906
25	SP, 124K, TOP COLL (TC), 2.8G	5708	83	SP,155K,100%,2.1G	7287
26	SP, 124K, TC, 2.6G	5478	84	SP,155K,105%,1.75G	6269
28	SP, 155K,-25%, 2.5G	4107	85	SP,155K,105%,2.1G	5545
29	SP, 155K,-25%, 3.4G	5036	86	SP,155K,100%,1.5G	6372
30	SP, 155K,-25%, 3.1G	4622	87	SP,155K,100%,1.85G	6495
31	SP, 155K,-25%, 3.1G	4993	88	SP,155K,100%,2.3G	8611
32	SP, 155K,-25%, 3.4G	7115			
35	LEFT CLIMBING TURN (LCT), 124K, 120% TORGUE (120%)	2685	36	RIGHT CLIMBING TURN (RCT), 124K, 120%	3466
39	LCT, 124K, 120%	4276	40	RCT, 124K, 120%	4335

18

C. DATA PROCESSING

1. Selection of Maximum and Minimum Loads

The data were received as a time array and a history array. A graphical representation of the data is given in Figure 2a through 2j and 3a through 3d. The maximum and minimum reversals were determined using a FORTRAN program, and the results were stored as a vector. The maximum loads were the principle focus of this study.

2. Assumptions Made in Processing the Data

In processing the data, the assumption was made that the experiments were correctly designed and the measurements were made accurately. In other words, the random signal inherent in a measuring process was designed to be insignificant compared with that of the load variable. This study did not focus on the data collection techniques. The data provided was taken to be a sample from the distribution of load of the symmetric pullout maneuver. The number of data measurements is the sample size.

3. Remarks About the Data

As noted in Table 1, each maneuver provided was not identical. There was replication of runs with respect to airspeed, but few replications of collective position and virtually no replication with respect to "g" loading. The top collective position seemed to indicate an increase in load levels as expected, but with only one top collective run

available, the effect of the variable was not studied. Increasing "g" loading also increased the level of loading as expected and influenced the load spectrum. In addition, the maximum load data were collected from two different flights: flight 37 and flight 43. The flights differed in gross weight and center of gravity location. As expected these differences greatly affected the loads seen by the component. The higher the gross weight the higher the maximum loads seen by the component.

III. STATISTICAL TREATMENT OF FLIGHT TEST DATA

A. HISTOGRAM AND ECDF OF FLIGHT TEST DATA

To draw conclusions about the population of loads on the basis of a sample of measurements taken on symmetric pullout maneuvers, the observed measurements were processed to display the properties of the sample that are relevant to the statistical analysis [Ref. 6]. Graphical means were used, specifically the loads histogram and the empirical cumulative distribution function (ECDF) of the maximum loads from 'RUN 23' and 'RUN 29' of the symmetric pullout maneuver. See Figures 4a/4b and 5a/5b. The histogram depicts the frequency that specified maximum load intervals were seen during a maneuver. Both runs, at two different airspeed indicate a large number of lower loads. The ECDF depicts the continuous nature of the loads. A significant cusp was evident which indicated the possibility of two populations in the data.

HIstogram: Run 23 Data
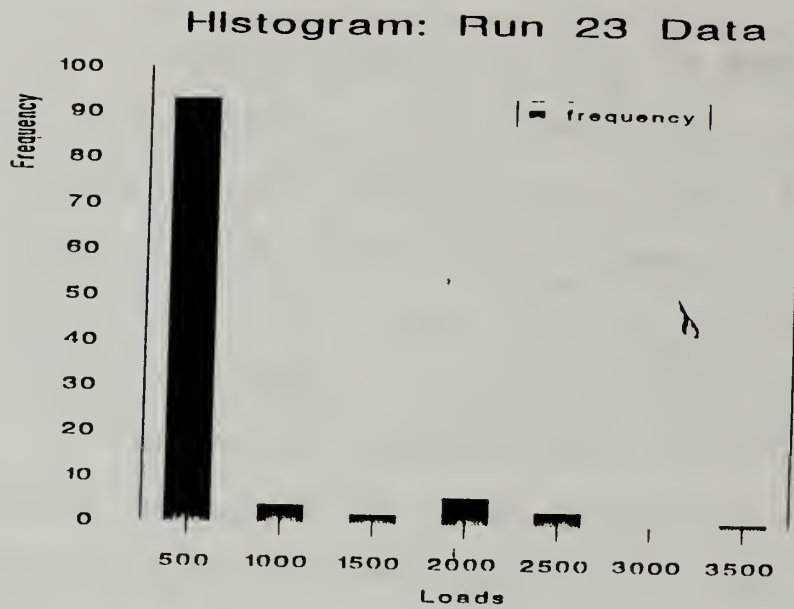
Figure 4a: Histogram of Run 23

ECDF: Run 23 Data
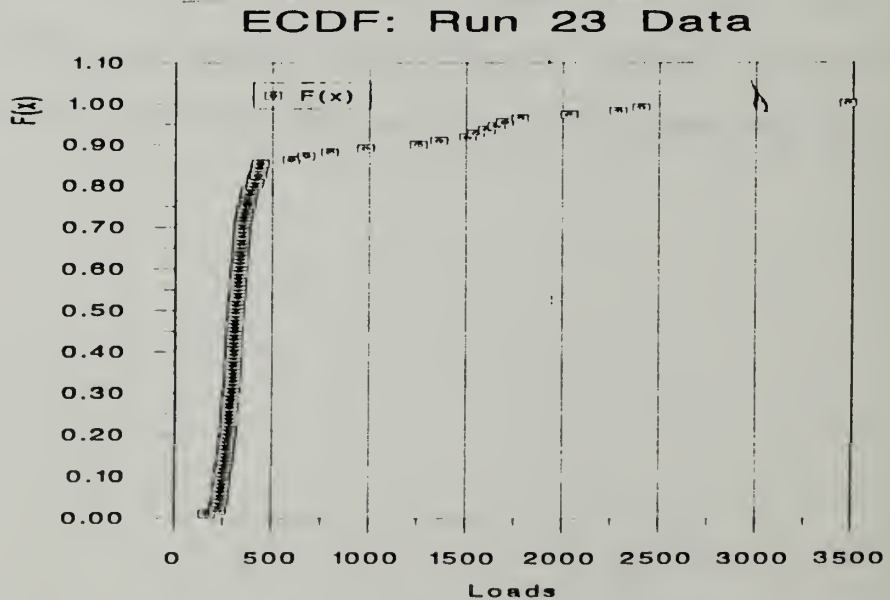
Figure 4b: ECDF of Run 23

22

Histogram: Run 29 Data

Figure 5a: Histogram of Run 29

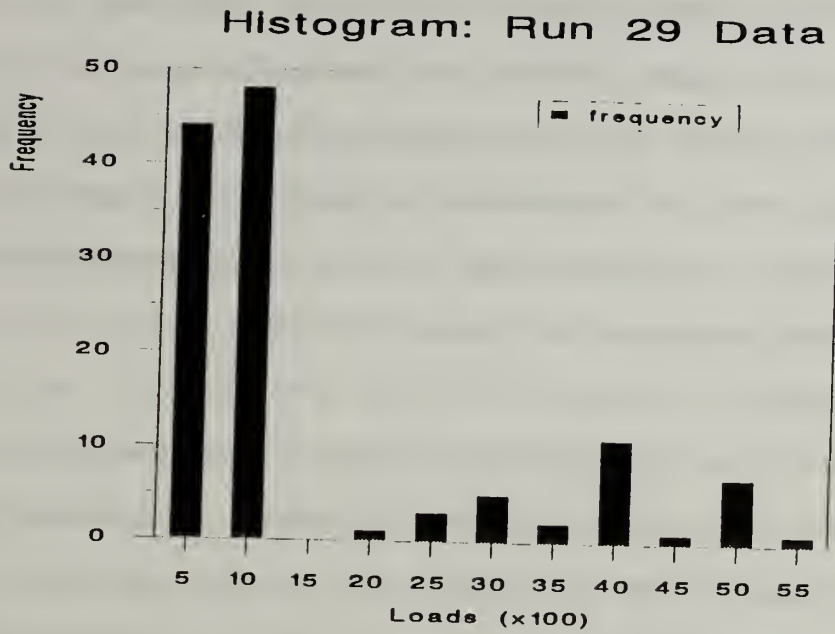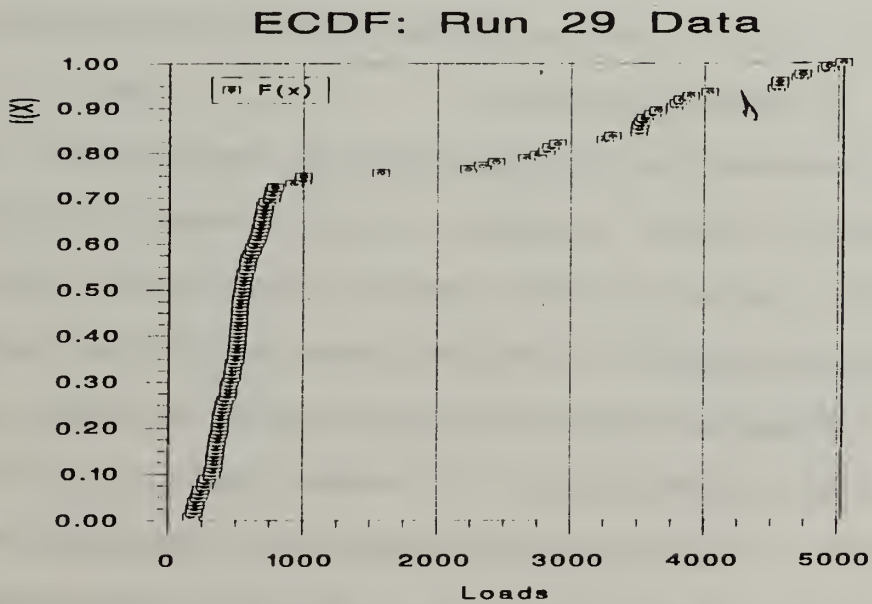# ECDF: Run 29 Data

Figure 5b: ECDF of Run 29

23

B. APPLYING PROBABILITY DISTRIBUTION FUNCTIONS

The aim of the statistical analysis was to construct a statistical model for the symmetric pullout load spectrum on the basis of the available incomplete information. The concept of a "model" is that it describes mathematically the probability aspect of a measurement variable.

1. AGSS

AGSS is a statistical program resident on the Naval Postgraduate School Mainframe Computer. This program is an advanced statistics program that can quickly and accurately process stochastic data. Among other things, it has the capability to fit numerous two parameter distributions using maximum likelihood estimation (MLE) to estimate for the parameters. It also provides four different goodness-of-fit statistics and the percentile data for each distribution fit.

2. Distributions Used

The sample size precluded a "brute force" fit of a mathematical curve directly to the frequency distribution. For this practice, the sample size would have to be considerably larger to yield reliable statistical conclusions.

Physical models form the basis of all well publicized probability distribution functions (pdf's). Rather than attempting to use physical arguments to determine the correct statistical distribution, five mathematical expressions were chosen to be compared to the data. The five distributions

24

were Normal, Weibull, Gamma, Lognormal and Exponential. (See Appendix A for a description of these distributions.) The data were fit to the distributions, and the goodness-of-fit measures were compared to determine which distribution best represented the data. The kurtosis and coefficient of variation were also used to determine the best distribution. In addition, the extreme value distribution was used to gain further understanding of the maximum load data.

3. Measure of Goodness-of-Fit

For this study the ability to quickly diagnose the goodness of fit by the AGSS was particularly useful. Of the four goodness-of-fit statistics provided by AGSS, the Anderson-Darling proved the most significant. (See Appendix B for a description of goodness-of-fit methods.)

4. Determining Cut-Off Loads

a. ECDF

Graphical interpretation of the histogram for RUNS 23 and 29, Figures 4a and 5a, indicate that the majority of the loads were measured during straight and level flight at the lower end of the load spectrum. The large kink in the ECDF's, Figure 4b and 5b, represented the possibility of two distinct populations in the data, the lower loads measured during the straight and level portion and the upper loads measured during the maneuver portion. Because it was the upper loads which were important to the calculation of damage,

a lower cutoff point needed to be determined. From the ECDF the cutoff point was determined by reading the load at the cusp. The cutoff point was estimated at 500 lbs for RUN 23, which was a conducted at 124 knots. The cutoff point was estimated at 1000 lbs for RUN 29, which was conducted at 155 knots.

b. Composite Goodness-of-Fit Plots

The load cutoff point was also evaluated using goodness-of-fit plots. Each of the 14 symmetric pullout runs were evaluated by selecting a range of cutoff points and fitting the data above them to the five distributions and comparing the goodness-of-fit results. See Figures 6a through 6n for the graphical representations. The y-axis is the goodness-of-fit statistic calculated using the Anderson-Darling method. The lower this statistic the better the fit. Note that the goodness-of-fit statistic for the maneuvers conducted at 124 knots differed from goodness-of-fit statistics for the maneuvers conducted at 155 knots. Nine runs conducted at 124 knots indicated an overall lower load cutoff point of 500 lbs. and the four runs conducted at 155 knots indicated a higher cutoff point of 1400 lbs.

Another observation was that one run, with the collective in the top position, followed neither the 124 knot population, at the fixed or -25 percent collective position, nor the 155 knot population. It was the only run with the top

26

collective position, so analysis of its characteristics was not possible except to say that it demonstrated significantly higher loads than the other nine runs at 124 knots. In conclusion two populations seemed to be evident, possibly three. Only the two populations involving the nine runs at 124 knots, with fixed or -25% collective, and the four runs at 155 knots were studied further.
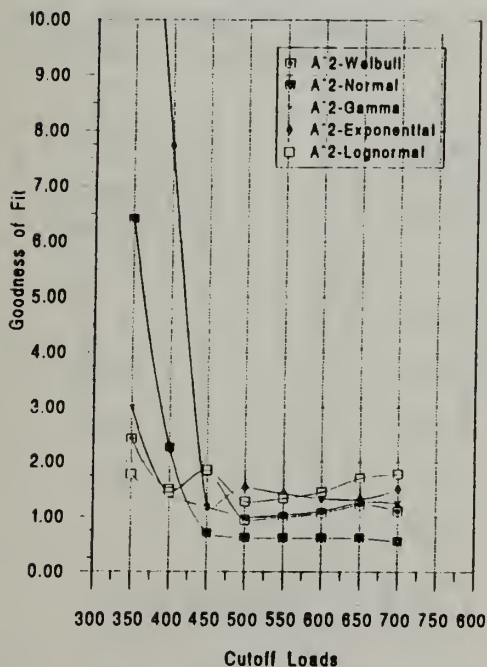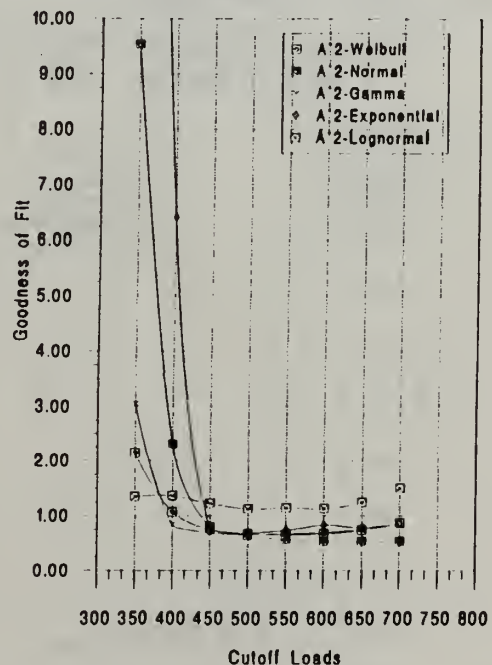
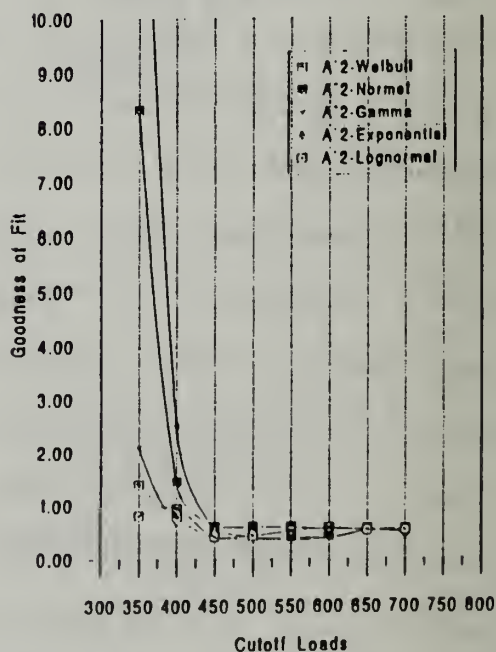Figure 6a - 6b
Evaluation of Cutoff Point Selection: Run 14, 15
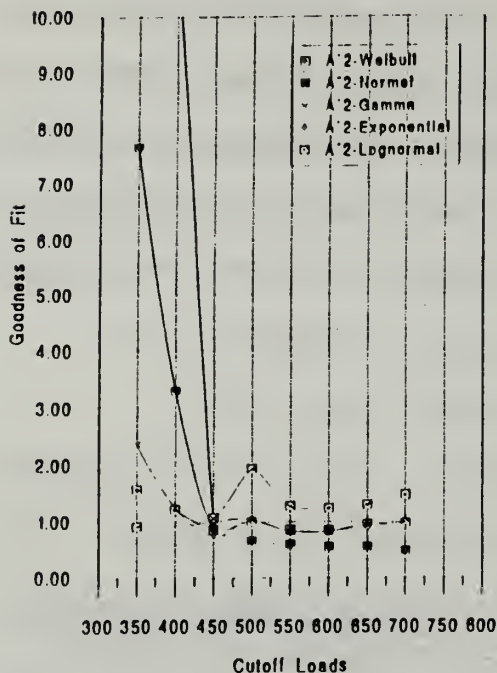
27
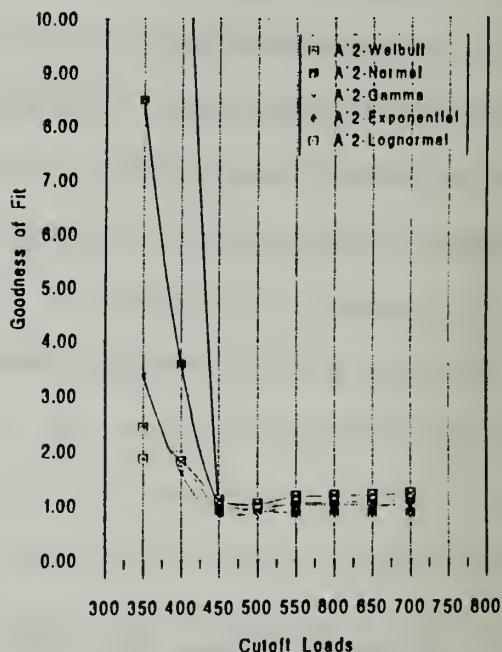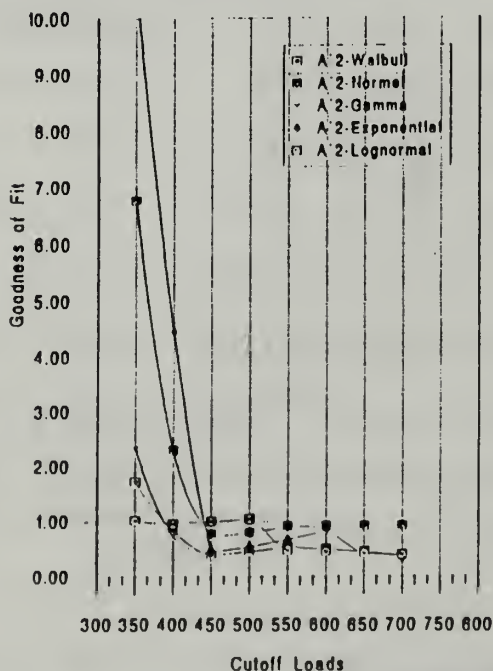
Figure 6c - 6f
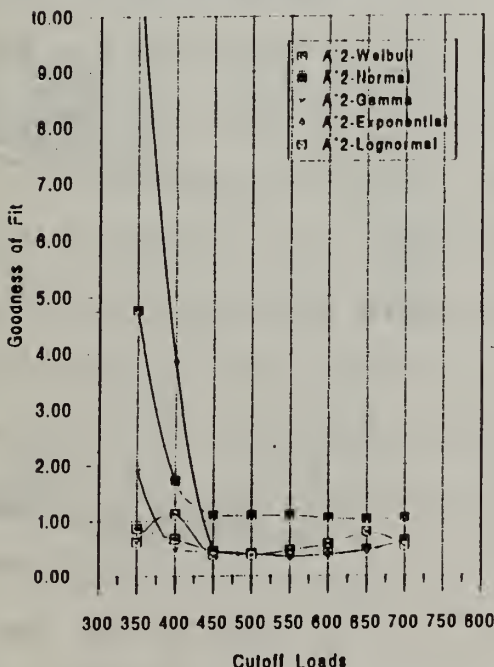Evaluation of Cutoff Point Selection: Run 16, 17, 19, and 21
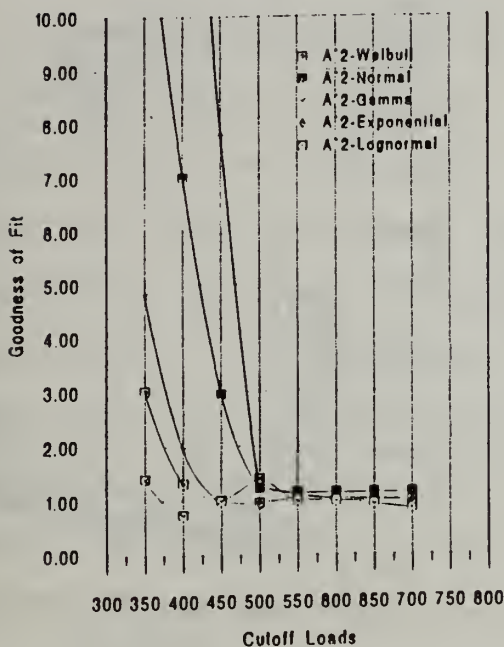
28
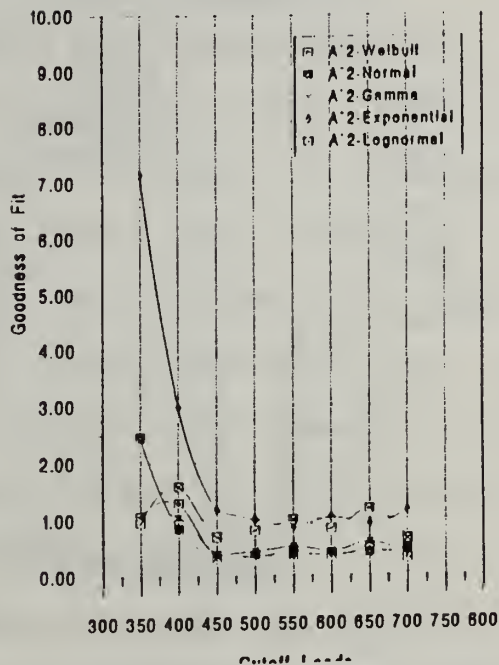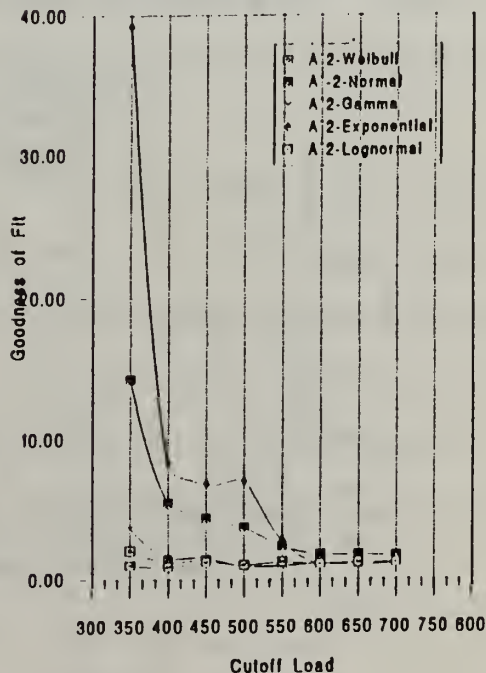
Figure 6g - 6j
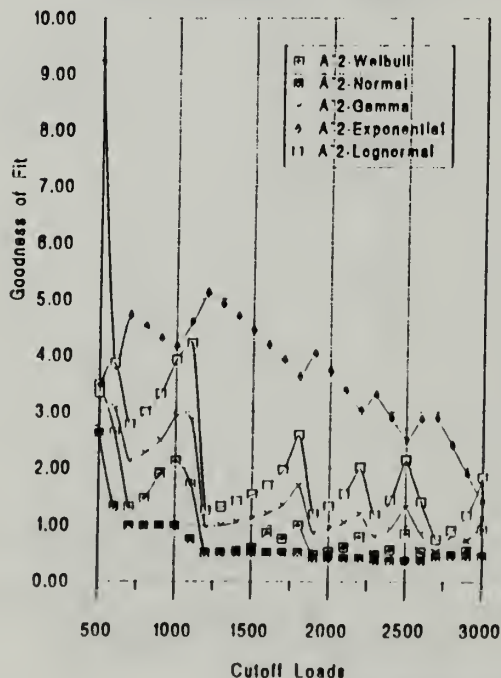Evaluation of Cutoff Point Selection: Run 22, 23, 24 and 25
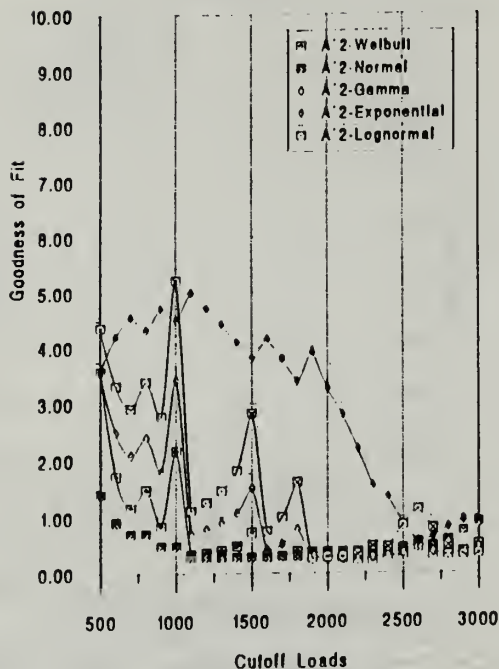
29
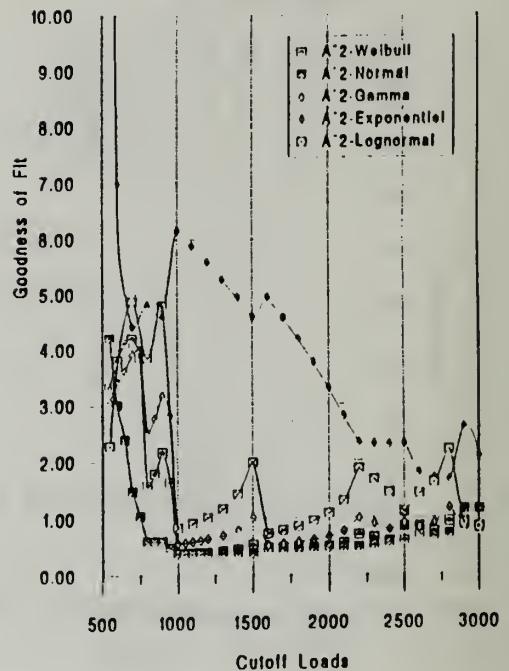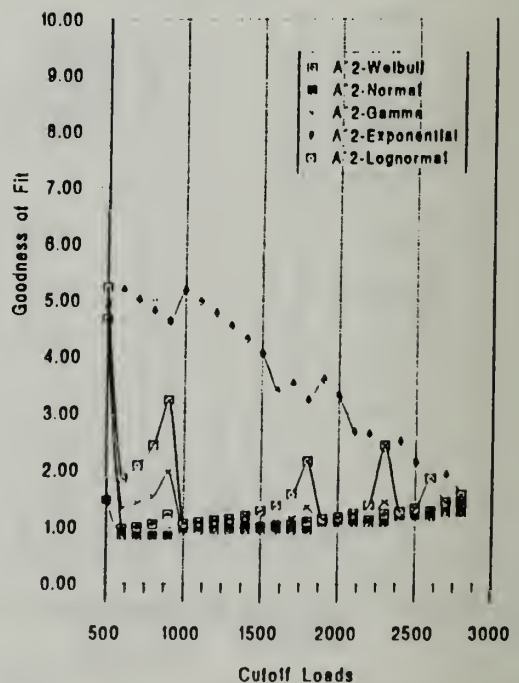
Figure 6k - 6n
Evaluation of Cutoff Point Selection: Run 28, 29, 30, and 31

30

C. SELECTING THE PROBABILITY DISTRIBUTION FUNCTION

1. Histogram and ECDF of Upper Load Populations

To draw statistical conclusions about the two populations, the data were again processed to see what properties of the upper load sample were amenable to statistical analysis. Graphical means were again used; specifically, the frequency of loads histogram and the empirical cumulative distribution function (ECDF) were plotted (Figure 7a/b for the 124 knot data and 8a/b for the 155 knot data). The histograms for the two airspeeds differ. The 124 knot histogram has a greater number of lower loads while the 155 knot histogram has a greater number of intermediate loads. The ECDF depicts the continuous nature of the loads. Bends or cusps are not evident, which provided evidence that the data were possibly from one population.

Because the sample size, i.e. the number of loads which represent the symmetric pullout, is variable, their distribution was also investigated (see Figure 9a for the 124 knot runs and Figure 9b for the 155 knot runs). From the 124 knot histogram the estimated expected number of loads was 17. From the 155 knot histogram the estimated expected number of loads was 26.
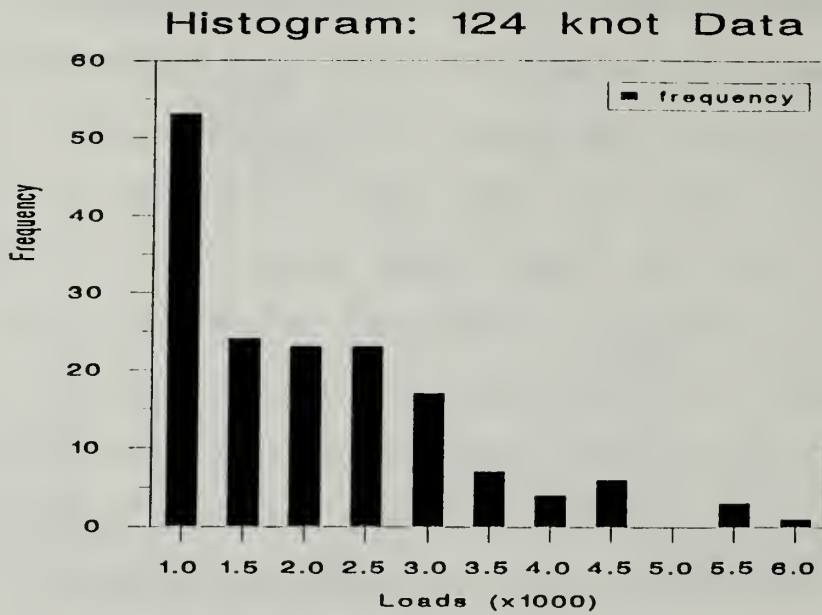
Figure 7a: Histogram of Upper Symmetric Pullout Loads, 124k
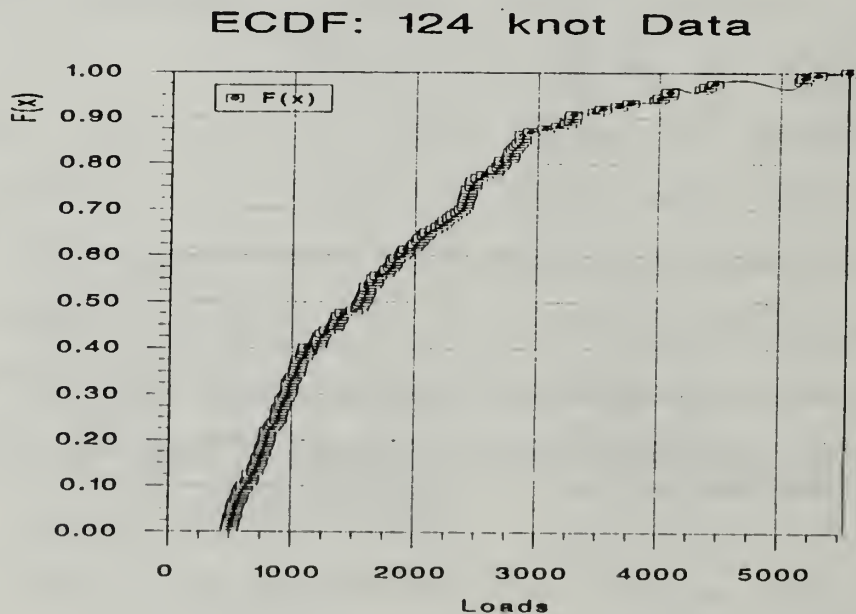
Figure 7b: ECDF of Upper Symmetric Pullout Loads, 124k

32

Histogram: 155 knot runs
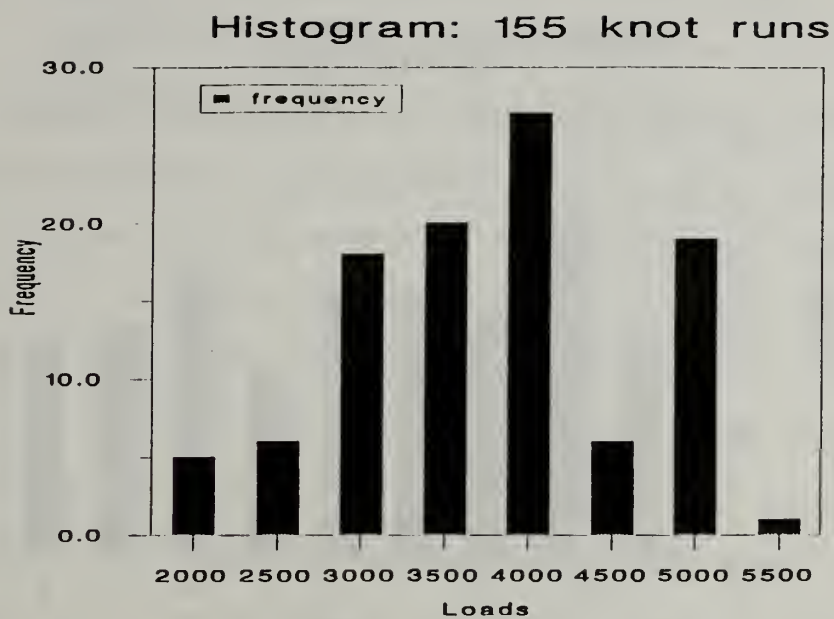
Figure 8a: Histogram of Upper Symmetric Pullout Loads, 155k

ECDF: 155 knot Data
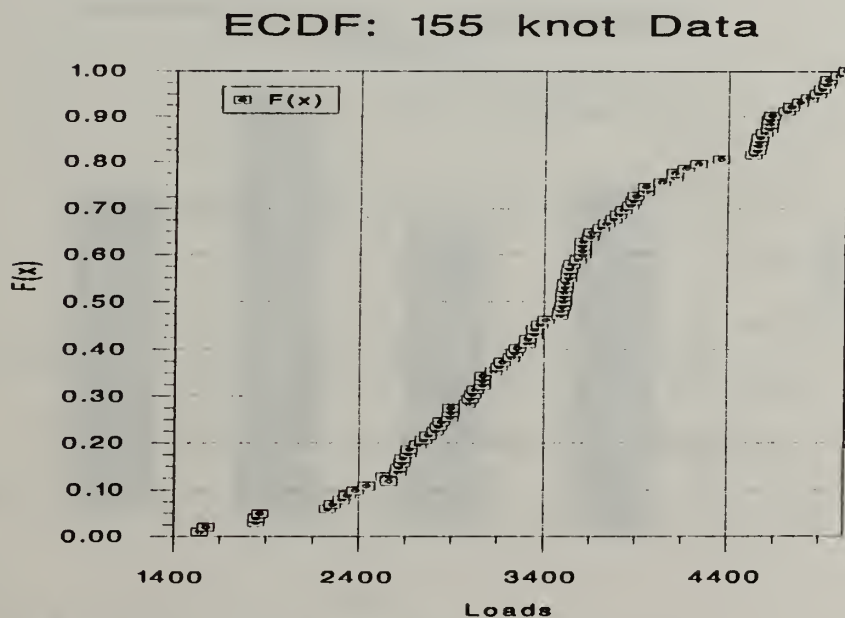
Figure 8b: ECDF of Upper Symmetric Pullout Loads, 155k

33
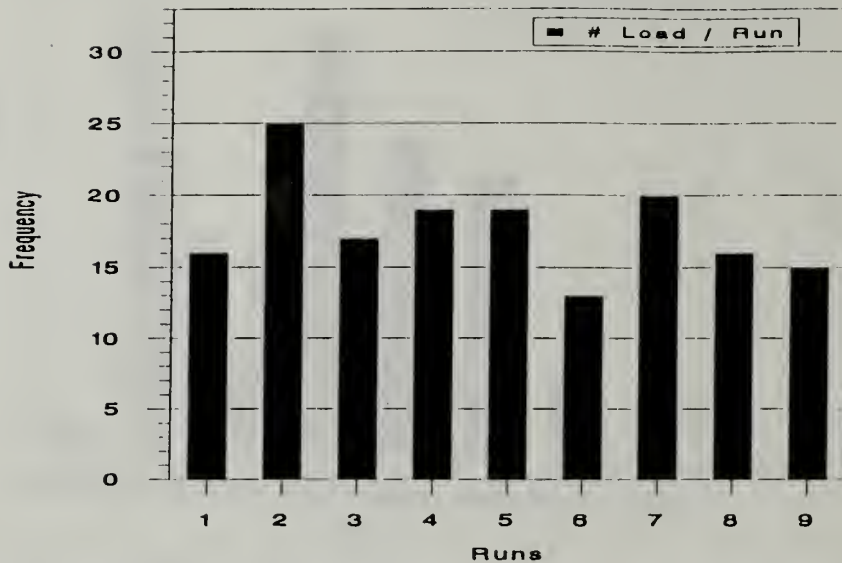
Figure 9a: Histogram of Upper Load Sample Size for Symmetric Pullout, 124 knot runs
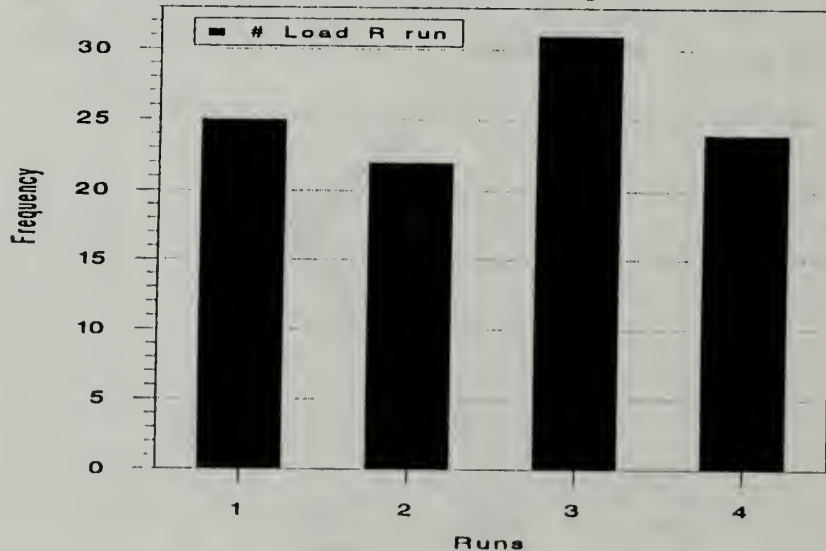
Figure 9b: Histogram of Upper Load Sample Size for Symmetric Pullout, 155 knot Runs

2. Skewness versus Coefficient of Variation

Only a few loads were observed for each run. The small amount of data made the comparison using goodness-of-fit measures somewhat inconclusive. From the comparison of distributions using goodness-of-fit statistics (see Figure 6a through 6m) all except the Exponential and the Lognormal provide a good fit to the data. To help in distribution selection, another method of comparison was used to gain better insight into the best choice to represent the distribution of loads for symmetric pullout. This comparison was made for two parameter distributions, by plotting the skewness versus the coefficient of variation. The general definitions of the two measures are

$$Skewness = \gamma_3 = \frac{E(X-\mu)^3}{\sigma^3}, \tag{2}$$

$$Coefficient\ of\ Variation = \gamma = \frac{\sigma}{\mu}, \tag{3}$$

for a random variable X with $\mu=E(X)$ and $\sigma^2=Var(X)$.

To illustrate, the Gamma Distribution, with shape parameter, r, and scale parameter, ß=1, has the following density.

$$f(v) = \frac{v^{r-1}e^{-v}}{\Gamma(r)} \qquad v \geq 0 \qquad\qquad (4)$$

The mean and standard deviation for this Gamma distribution are given by:

$$\mu = \int_0^\infty \frac{v^r e^{-v}}{\Gamma(r)} dv = \frac{\Gamma(r+1)}{\Gamma(r)} = r, \qquad\qquad (5)$$

$$\sigma^2 = \int_0^\infty (v-\mu)^2 \frac{v^{r-1}e^{-v}}{\Gamma(r)} dv = (r+1)r - 2\mu r + \mu^2 = r, \qquad (6)$$

from which the coefficient of variation can be calculated to be:

$$\gamma = \frac{\sigma}{\mu} = r^{-.5}. \qquad\qquad (7)$$

To find the skewness is found to be

$$E(X-\mu)^3 = \int_0^\infty (v-\mu)^3 \frac{v^{r-1}e^{-v}}{\Gamma(r)} dv = (r^3 + 3r^2 + 2r) - 3\mu(r^2+r) + 3\mu^2 r - \mu^3 = 2r.$$
$$(8)$$

Thus,

$$\gamma_3 = \frac{2r}{r^{1.5}} = 2r^{-.5} = 2\gamma. \qquad\qquad (9)$$

With such expressions, kurtosis can be plotted versus the coefficient of variation for each distribution. A composite plot in Figure 10 shows the relationships for all the distributions used. Note the x axis represents the Normal Distribution, as the skewness is zero. Comparing the skewness to the coefficient of variation for each load sample indicates by which distribution (Weibull, Lognormal, Gamma, Exponential) the sample can be reasonably represented. [Ref. 9]   See Figure 11 for the 124 knot runs and Figure 12 for the 155 knot runs.   From this comparison, the Weibull distribution was chosen as the best model for both populations.

Comparison of Distribution
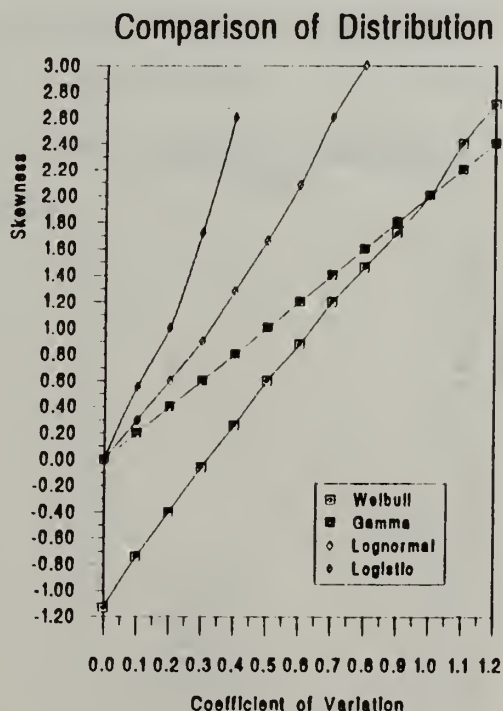
Figure 10: Skewness versus Coefficient of Variation Comparison

37

Comparison of Distribution: 124
knots
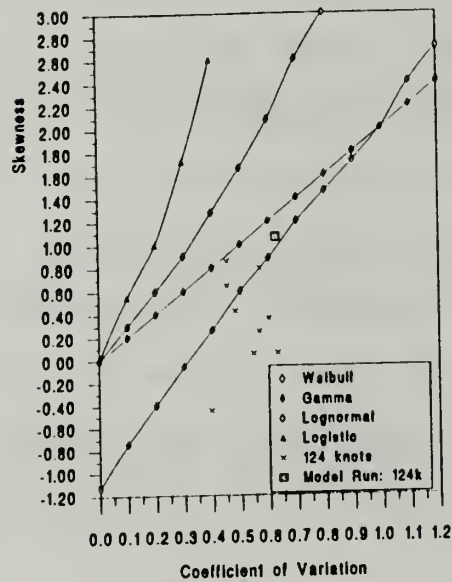
Figure 11: Comparison of Distribution, 124k Data

Comparison of Distribution: 155
knots
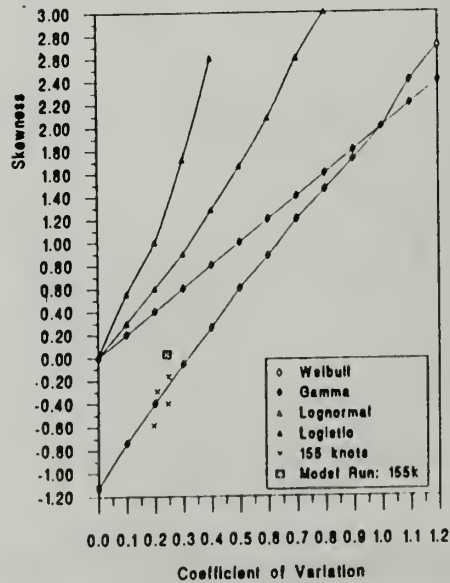
Figure 12: Comparison of Distribution, 155k Data

38

3. Statistical Model of Symmetric Pullout

a. Determine Weibull Parameters

Once the Weibull distribution was chosen, the data from the individual symmetric pullout runs, were used to estimate the distribution parameters at both 124 and 155 knots. Both data sets provided a good fit as reflected by the Anderson-Darling goodness-of-fit test. See Figure 13 and 14, for comparisons of the data histogram with the estimated Weibull density, the ECDF with the estimated Weibull cumulative distribution and a plot of the raw data percentiles with the estimated Weibull percentiles. The shape parameters for the 124 knot runs and the 155 knot runs were estimated to be 1.03 and 2.66 respectively. The scale parameters for the 124 knot and 155 knot runs were estimated to be 1331.9 and 2331.9 respectively.

WEIBULL DENSITY FUNCTION, N=160

WEIBULL CUMULATIVE DISTRIBUTION FUNCTION, N=160

WEIBULL PROBABILITY PLOT, N=160

PERCENTILES	SAMPLE	FITTED
5:	44.4	75.091
10:	140.6	150.75
25:	395.95	398.66
50:	1079.5	934.04
75:	1972	1827.3
90:	2784.5	2986.5
95:	3579	3853.1
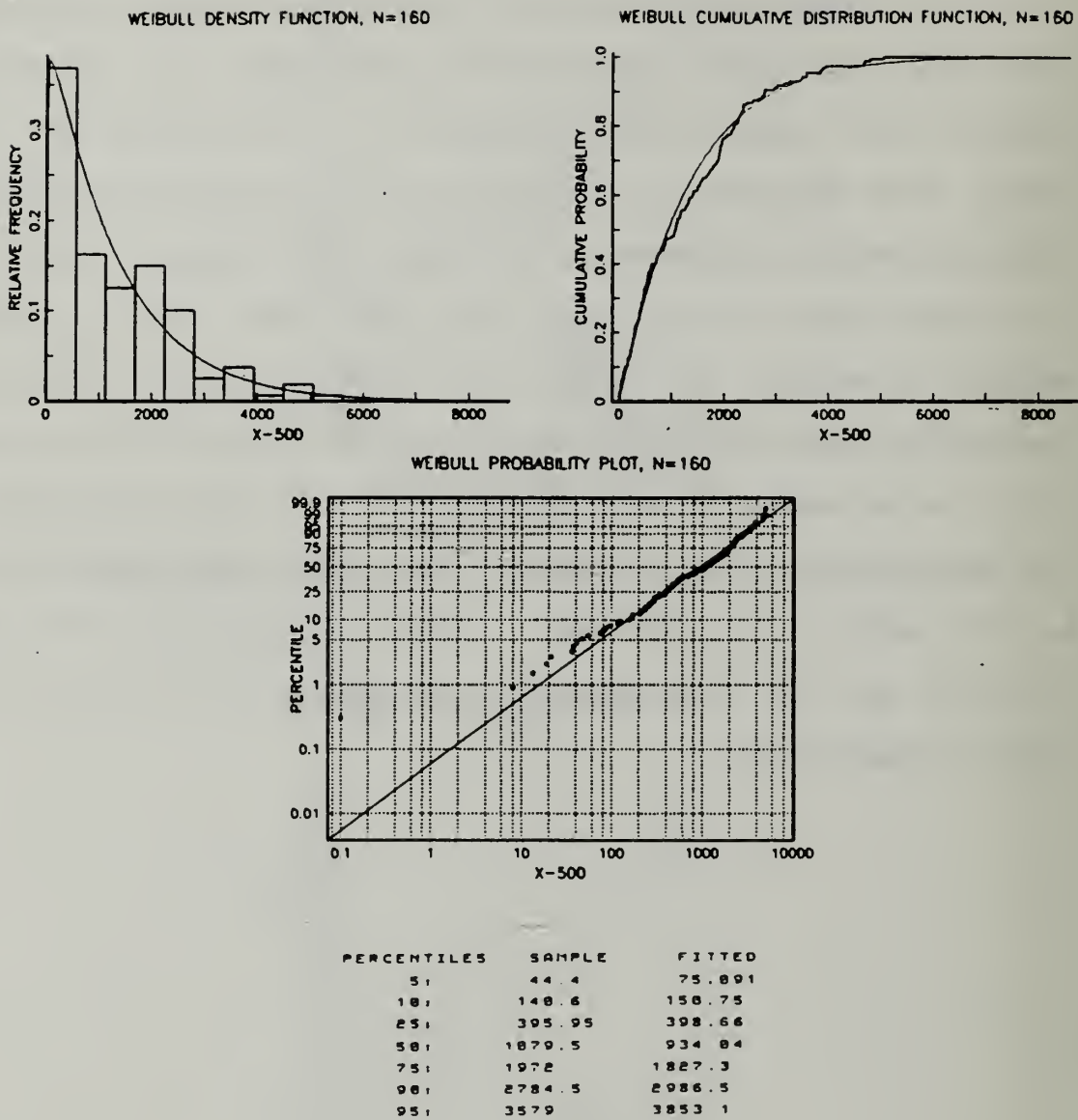
Figure 13: Weibull Distribution, 124k
pdf, CDF, Probability, Percentiles

40

WEIBULL DENSITY FUNCTION, N=102

WEIBULL CUMULATIVE DISTRIBUTION FUNCTION, N=102

WEIBULL PROBABILITY PLOT, N=102
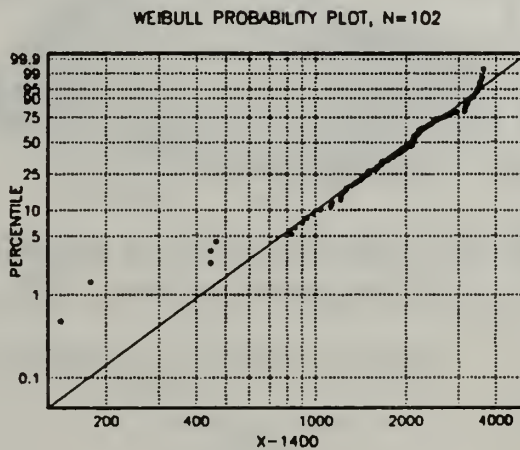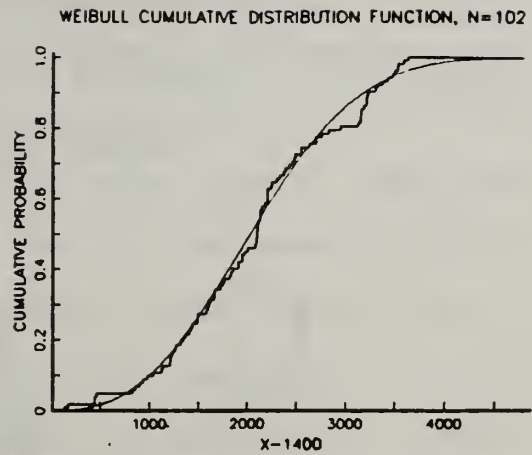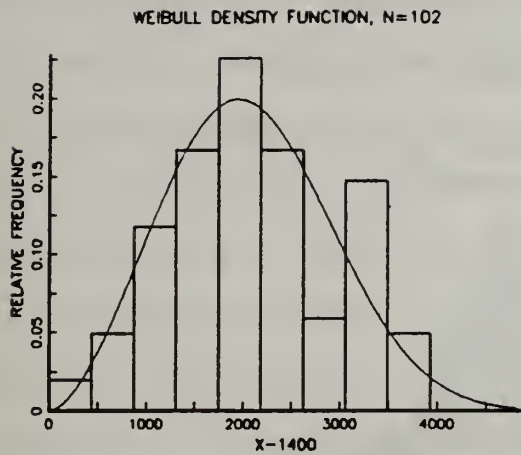
PERCENTILES	SAMPLE	FITTED
5:	832	764.83
10:	1041	1081.3
25:	1493	1468.2
50:	2106	2031.8
75:	2638	2636.1
90:	3232	3189.6
95:	3482	3521

Figure 14: Weibull Distribution, 155k
pdf, CDF, Probability, Percentiles

Maximum likelihood estimation finds the parameters which maximizes the likelihood of observing the actual sample values. These likelihoods, which are a function of the parameters, are plotted in Figure 15 and 16.

WEIBULL LIKELIHOOD SURFACE ($\times 10^{568}$)
N=160
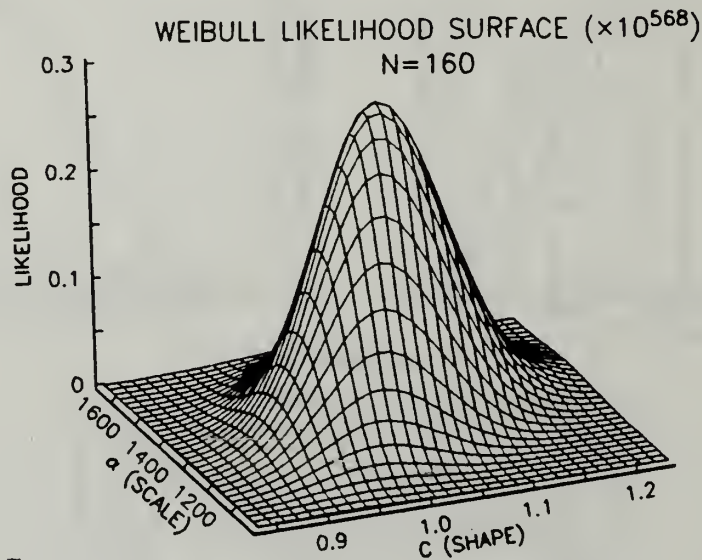
Figure 15: Maximum Likelihood Estimation (MLE), 3D Representation, 124k

WEIBULL LIKELIHOOD SURFACE ($\times 10^{361}$)
N=102
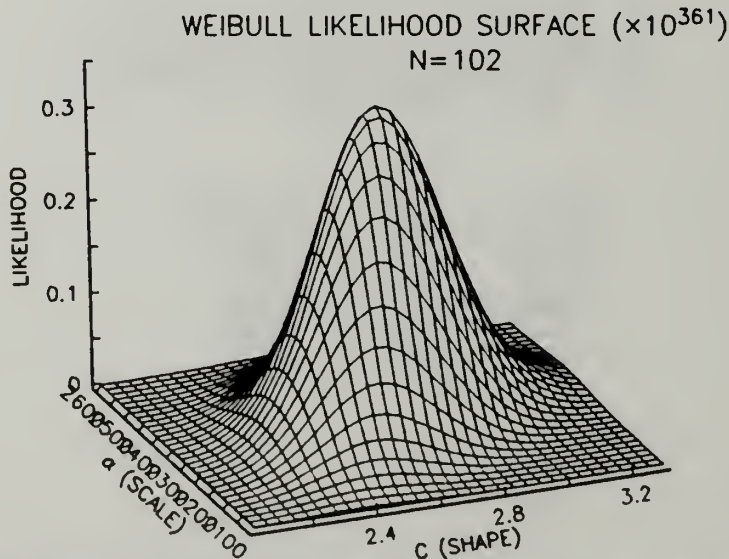
Figure 16: Maximum Likelihood Estimation (MLE), 3D Representation, 155k

b. Uniform Distribution Check

The shape and scale parameters for the Weibull distribution were estimated from the pooled data. The fit to this Weibull distribution was evaluated using the Anderson-Darling goodness of fit test for each individual run. If in fact, the Weibull distribution is the correct underlying distribution for each run, then the P-values associated with the Anderson-Darling goodness-of-fit test should have a Uniform distribution. This is a consequence of the probability integral transformation. Therefore, the overall goodness-of-fit can be evaluated by looking at the distribution of P-values. See Figure 17 for the 124 knot runs, and Figure 18 for the 155 knots runs. From these figures the P-values were uniformaly distributed, thus even considering the data as a whole there is still no evidence of lack of fit to the Weibull distribution.
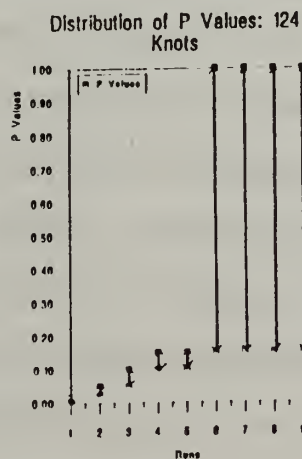
Figure 17: Uniform Distribution of Individual Run Compared to Model Run, 124 knots

Distribution of P Values: 155 Knots
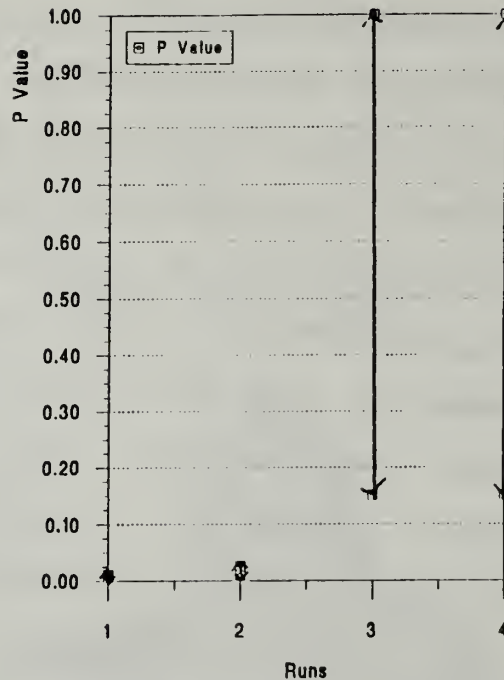
Figure 18: Uniform Distribution of Individual Run
Compared to Model Run, 155 knots

c. **Weibull Model for 124 knot and 155 knot data**

Using the percentiles from the fitted cumulative

distribution function for the 124 knot runs and the estimated

expected sample size per run, 17, the model load spectrum was

determined. The same procedure was conducted for the 155 knot

runs and estimated expected sample size per run was 26. The

maximum load of the 155 knot, 'plot 2.0' substantiation run

was approximately the 87th percentile load of the 155 knot

model run. A comparison of the 124 knot data cannot be made

because no substantiation run was provided for this airspeed.

D. EXTREME VALUE STATISTICS

1. Maximum Load Populations

The maximum load data was also processed to attempt to understand the overall symmetric pullout distribution. See Figure 19 and 20 for a depiction of the maximum load values at 124 knots, excluding the top collective, and at 155 knots. Note the difference in maximum loads due to the effects of increased gross weight, as the gross weight increased the maximum loads increased. Flight 37 was flown at 16,500 lbs. gross weight. Flight 43 was flown at 20,800 lbs. gross weight. The x-axis represents the number of data points available for each airspeed and gross weight.

For an extreme value distribution, the number of maneuvers (n) crucially influences both the location and scale parameters. This feature is important because the distribution of the maximum value shifts toward the right as the sample size (n) is increased. The number of maneuvers needed to represent the overall maximum load distribution was fixed at 20 as this was the number of times the symmetric pullout maneuver (155 knots and over 2.0 g's) was performed in 100 hours, as determined by Sikorsky's loading spectrum (see Table 1). With no other data available, the assumption was made that all symmetric pullout maneuvers would also be performed 20 times in 100 hours.

45
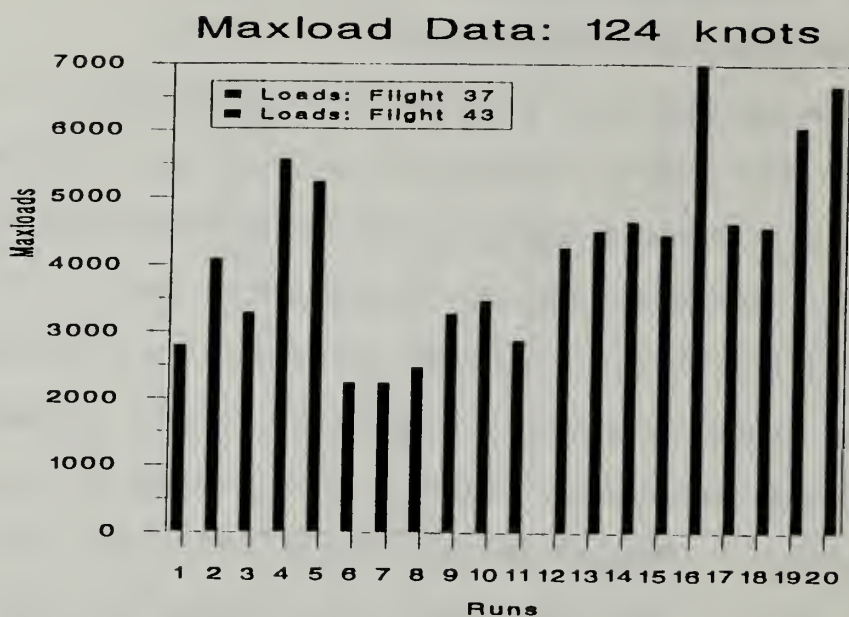
Figure 19: Maximum Load Data at 124 knots
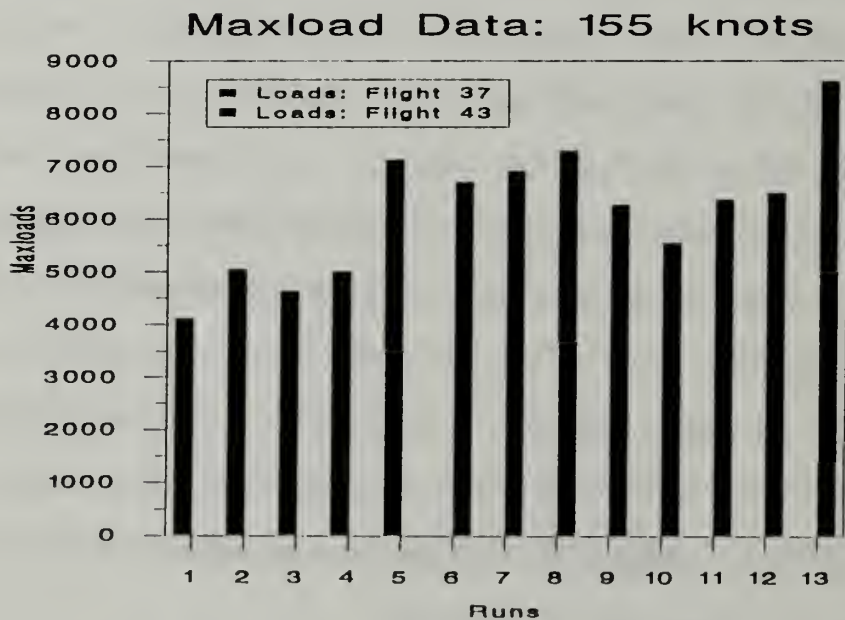
Figure 20: Maximum Load Data 155 knots

46

2. Fits to Extreme Value Distribution

The maximum data points were fit to a 'type I' extreme value distribution. The 'type I' extreme value distribution arises from the distribution of the maximum of a sample of size n for an initial distribution that is unbounded in the direction of the extreme value. This is true for the symmetric pullout data [Ref. 10]. For large sample sizes the maximum extreme value from a Normal, Lognormal, Gamma, and Weibull distribution can be modeled by a 'type I' distribution [Ref. 11]. The equation for the Extreme Value distribution is found in Table A.1 in Appendix A. Figure 21 depicts the extreme value fit of 20 symmetric pullout maximum data points at 124 knots for both gross weights. The probability plots were made to visually evaluate the fit. In addition, the percentiles of the sub-populations were prepared for comparison. Figure 22 looked at the 9 lower gross weight extreme value points at 124 knots. Note: only 9 were available. Figure 23 depicts the extreme value fit of 13 of the symmetric pullout maximum data points at 155 knots for both gross weights. Note: only 13 values were available. Figure 24 shows four of the lower gross weight extreme value points at 155 knots. Note: only four were available. All four sub-populations indicate a good fit using the Anderson-Darling goodness-of-fit tests. Because 20 data points were not available for each sub-population, the curves were shifted

47

to the left making the overall results slightly less conservative. Note the extreme value percentiles with the combined lower and higher gross weight have much larger loads than the percentiles of just the lower gross weight. For example the 124 knot, combined gross weight fitted 95th percentile value was 6498.3 lbs.; while just the lower gross weight 124 knot sample was 5087.7 lbs. The same comparison was made of the 155 knot data. The combined gross weight sub-population fitted 95th percentile was 8061.8 lbs., while the lower gross weight fitted 95th percentile was 7001.8 lbs.

The extreme value percentiles were used to understand where the model and substantiation runs fell in the overall population of symmetric pullout data. The model 124 knot symmetric pullout 95th percentile was 4353.1 lbs. This represents only a 78th percentile load for the lower gross weight, 124 knot extreme value model. The model 155 knot symmetric pullout 95th percentile was 4921.0 lbs. This represents about a 45th percentile load for the lower gross weight, 155 knot extreme value model. The maximum load of the 155 knot substantiation run conducted at gross weights between 19,000 and 21,000, was 4490 lbs. This represents only a 20th percentile in the combined gross weight extreme value distribution and a 45th percentile load for the lower gross weight 155 knot extreme value model. The maximum load for the substantiation run was expected to be at the 50th percentile

48

or higher in the extreme value model, because the substantiation run was the highest load run out of the four to five substantiation runs conducted by Sikorsky.

EXTREME VALUE PROBABILITY PLOT, N=20

PERCENTILES	SAMPLE	FITTED
5:	2232	887.85
18:	2355	1888.8
25:	3874.5	3266.3
58:	4364	4479.3
75:	5394	5435.4
98:	6365	6135.3
95:	6834	6498.3
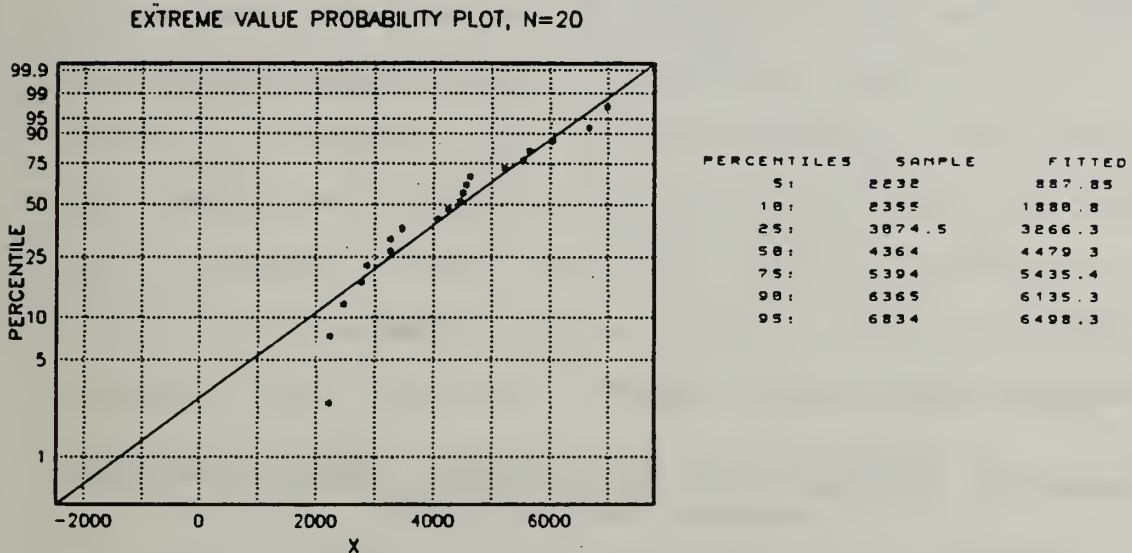
Figure 21: Extreme Value Distribution, Symmetric Pullout, Maximum Load Data 124k

EXTREME VALUE PROBABILITY PLOT, N=9

PERCENTILES	SAMPLE	FITTED
5:	2227	528.95
18:	2227	1329.1
25:	2783	2456.9
58:	3276	3444.3
75:	3472	4222.5
98:	5555	4792.2
95:	5555	5887.7
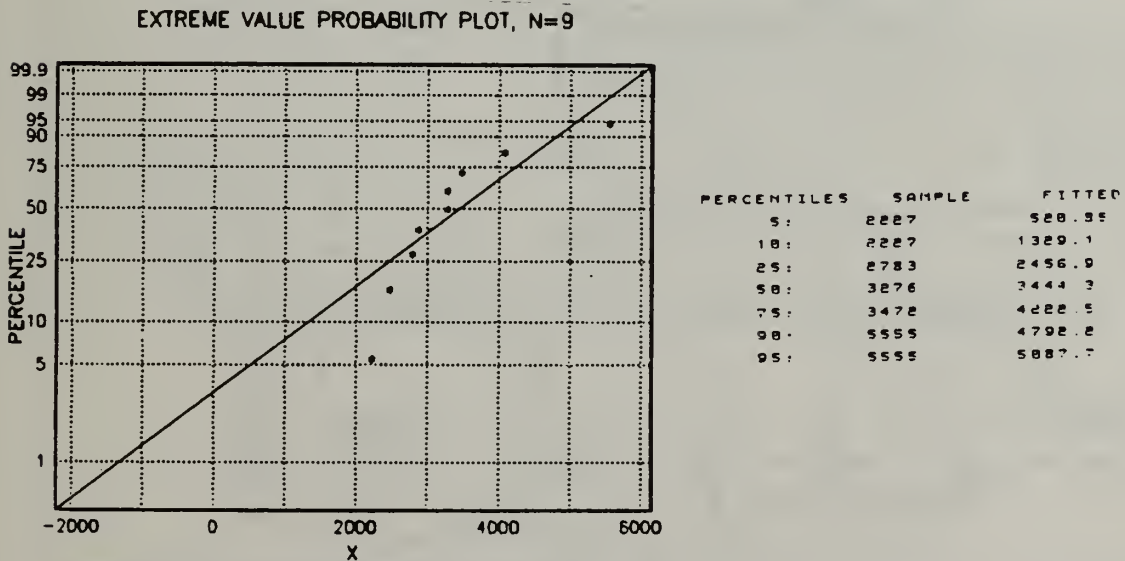
Figure 22: Extreme Value Distribution, Symmetric Pullout, Maximum Load Data, 124k, Flight 37: Lower Gross Weight

49

EXTREME VALUE PROBABILITY PLOT, N=13
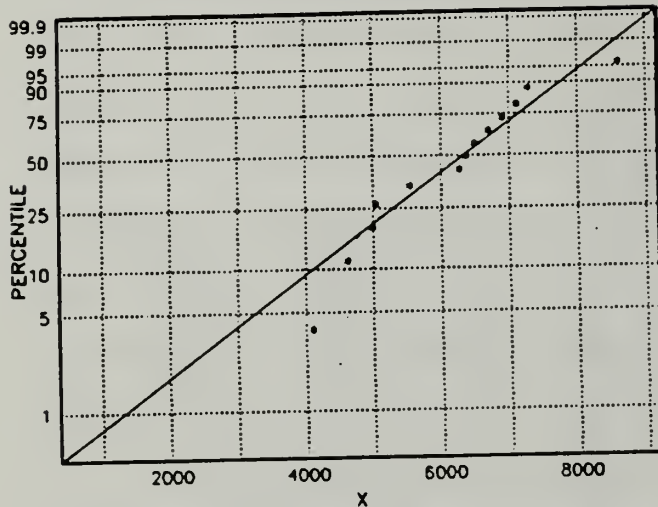
PERCENTILES	SAMPLE	FITTED
5:	4187	3258.3
10:	4622	4101.8
25:	5036	5298
50:	6372	6338.2
75:	6386	7150.1
90:	7287	7758.3
95:	8611	8861.6

Figure 23: Extreme Value Distribution, Symmetric Pullout, Maximum Load Data 155k

EXTREME VALUE PROBABILITY PLOT, N=5
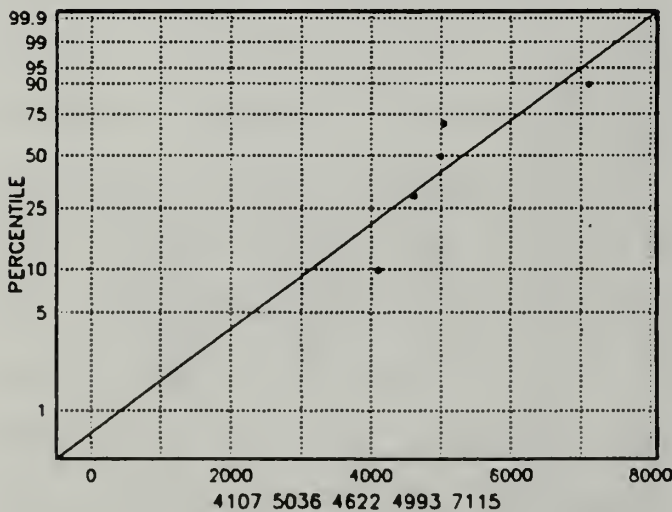
PERCENTILES	SAMPLE	FITTED
5:	4187	2388
10:	4187	3138.7
25:	4622	4297.9
50:	4993	5312.7
75:	5036	6112.6
90:	7115	6698.1
95:	7115	7881.8

Figure 24: Extreme Value Distribution, Symmetric Pullout, Maximum Load Data, 155k, Flight 37: Lower Gross Weight

50

IV.   FATIGUE ANALYSIS

A.   PART DESCRIPTION

The servo beam rail is a fatigue critical component loaded by the main rotor forward longitudinal servo star (MRFLSS). The MRFLSS is part of the flight control servo which directly connects the mixing unit to the swashplate.   The hydraulic servo tilts the swashplate assembly, which moves the control rods attached to each spindle, directly controlling the movement of the rotor blades.   Figure 25 is a dimensioned drawing of the component.   Figure 26 shows how the star, or swashplate loads are applied to the component.
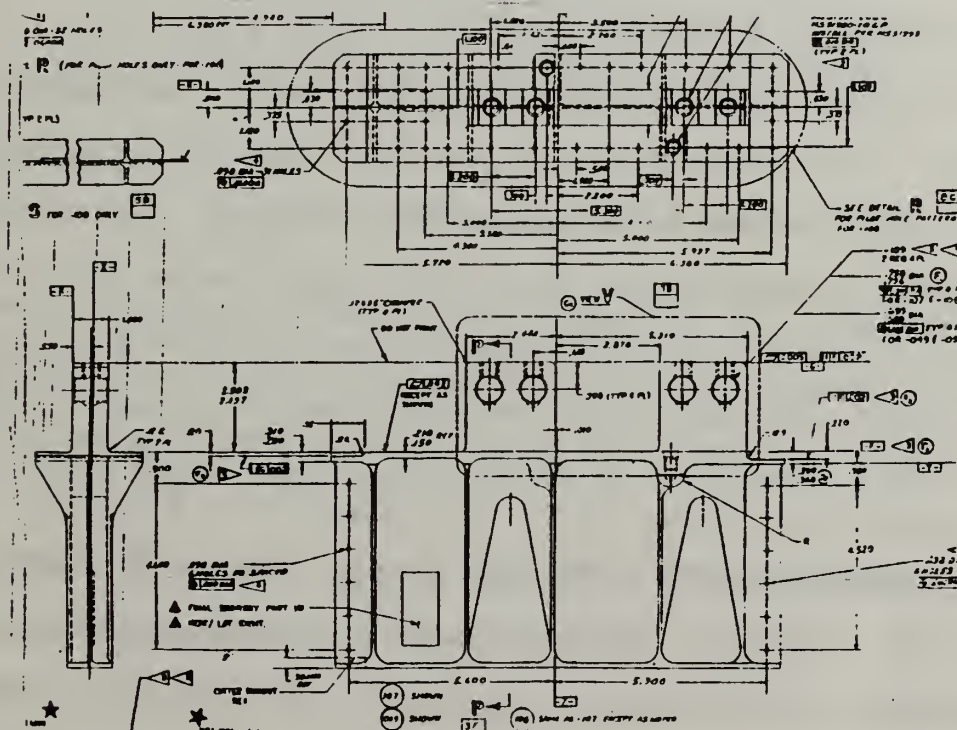
Figure 25: Dimensioned drawing of Servo Beam Rail, 048

51

STAR LOAD 2 / 1.1

STAR LOAD 1 / 1.1

BEAM POSITION 1

SERVO 2

BEAM POSITION 2

SERVO 1

BEAM POSITION 3
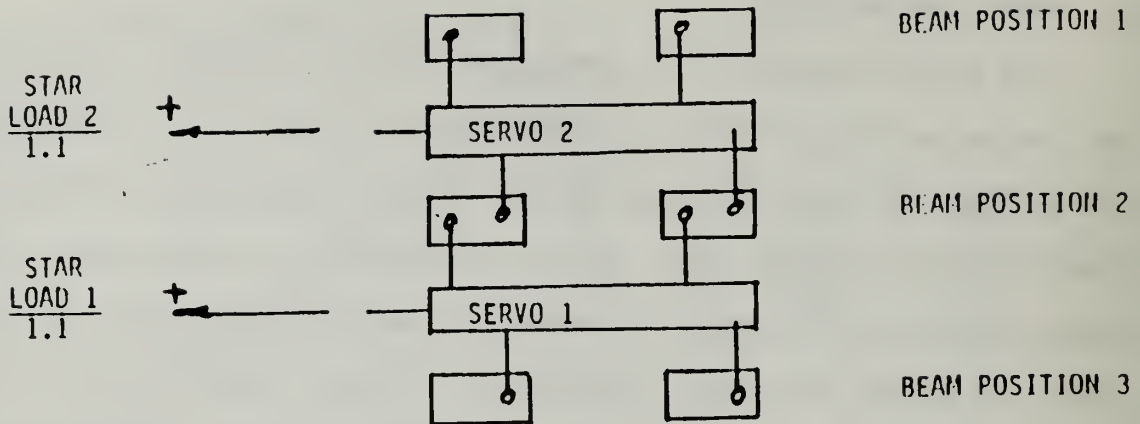
Figure 26: Application of Star loads on the Component

B. METHOD OF ANALYSIS

The safe life fatigue analysis method was used in this study. The maneuver spectrum used was the proposed usage spectrum provided by Sikorsky (see Table 1). It included all critical maneuvers the helicopter experienced in 100 flight hours during its intended design mission. The loads spectrum developed previously was used with the component S-N curve to calculate damage for a symmetric pullout using Miner's rule.

C. DETERMINING THE COMPONENT STRESS LIFE (S-N) CURVE

The component maximum load S-N curve method used by Sikorsky originally was utilized during this study to calculate the damage of the component. The servo beam rail

52

was constructed of unchaffed aluminum. To avoid full scale
component tests, Sikorsky used the specimen unchaffed
aluminum, S-N curve shape for the component S-N curve shape
[Ref. 4]. See Figure 27 and Equation 4.
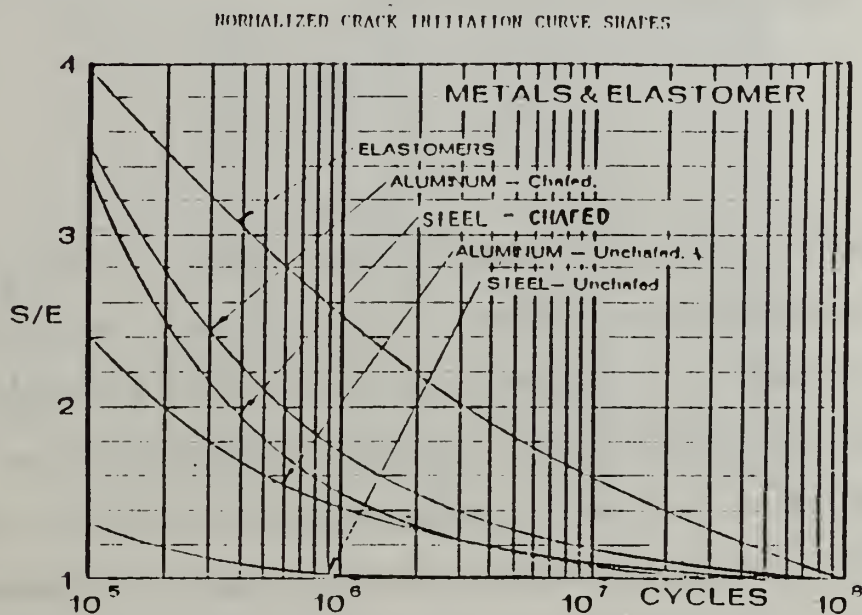
Figure 27: Material S/N Curve

Laboratory fatigue tests were completed by Sikorsky with
steady and oscillatory loads applied to the component. Due to
time and expense of testing, it was not possible to fail each
part. In this case runouts at load levels high enough to
guarantee a component life in excess of an established design
goal were considered acceptable test points. For this
component, three tests indicated failure or significant

53

runout; thus, the substantiation of the S-N curve was based on only three test data points. The endurance limit for a given mean load for the individual test data points was calculated using Equation (10) and the values of the endurance limits ($S_{max\ infinity}$) were averaged.

$$\frac{S}{S_{max\ \infty}} = 1 + \frac{\beta}{N^\gamma} \tag{10}$$

The maximum of the three oscillatory loads (S), which caused damage or significant runout, were 6500 lbs., 8810 lbs., and 8500 lbs. [Ref. 4]. The mean loads for these vibratory loads were 3250 lbs., 2200 lbs., and 2200 lbs., respectively [Ref. 4]. The gamma and beta, curve shape constant of Equation (10), for unchaffed aluminum were .5 and .483 respectively [Ref. 4]. The average endurance limit calculated from (10) was determined to be 4971 lbs. The "working" maximum load S-N curve was obtained from the experimental S-N curve through multiplication by the Reliability Reduction Factor, which equalled .61 in this case. The resulting reduced endurance limit was 3032 lbs. This reduction factor was obtained from previous tests by Sikorsky. The resulting component S/N curve equation is given in Equation (11).

$$S_{\max} = (.61)4971(1 + .\frac{483}{\sqrt{N}}) \qquad\qquad (11)$$

The resulting curve is depicted in Figure 28.
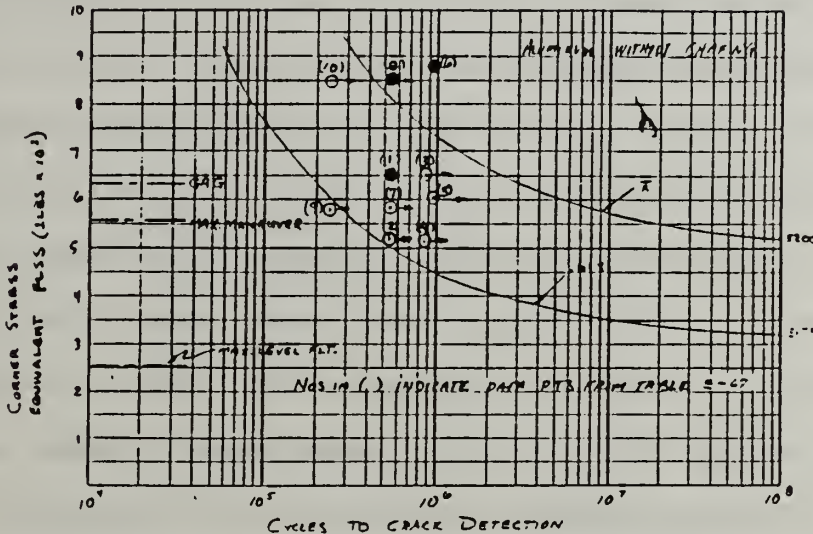
Figure 28: Component S/N Curve

D. DAMAGE AND LIFE CALCULATIONS

1. Miner's Rule

Once the loading sequence, the load reversals, and the maximum load component S-N curve were determined, crack initiation times were calculated using linear cumulative damage theory in order to determine a safe life replacement time. The damage calculations were first made for each maneuver and then expressed in terms of damage per 100 hours. Fatigue damage accrued for each of the spectrum loads was calculated using equation (12).

55

$$\text{Damage per 100 hours} = \frac{n}{N} \qquad\qquad (12)$$

The "n" is the anticipated number of cycles at a given maximum load to be experienced in 100 hours and "N" is the allowable cycles at the same load level, in millions, as defined by the component S-N curve. Damage was only caused by maximum loads greater than the endurance limit. The damage calculation for each load was multiplied by the frequency of maximum loads in the maneuver. This value was then multiplied by the occurrences, or number of times the maneuver would be performed during 100 hours as specified by the maneuver spectrum. The recommended replacement time was equal to the calculated summation of damage for each maneuver during 100 hours rounded off to the nearest two significant figures.

2. Interval Sizing

The maximum loads were sorted into intervals for future damage calculations. Two methods were used to determine the interval size. The first interval division was provided by NAVAIR as Sikorsky's method of interval sizing [Ref. 11]. It was based on the endurance limit (endl). The interval sizing was:

```
0.75 x endl - 1.00 x endl
1.00 x endl - 1.25 x endl
1.25 x endl - 1.50 x endl
1.50 x endl - 1.75 x endl
1.75 x endl - 2.00 x endl
```

The designated load level used for each interval was calculated as:

.6 ((0.75 x endl) - (1.00 x endl)) + (0.75 x endl).

The .6 factor resulted from a previous study be Sikorsky. The second method of sorting was based on the interval sizes taken directly from Sikorsky's fatigue analysis for this particular maneuver [Ref. 4]. They were:

```
2000 - 2110
2110 - 2700
2700 - 3290
3290 - 3880
3880 - 4460
4460 - 5050
5050 - maximum load
```

3. Damage Comparisons

Damage calculations were completed on the 13 runs of the original symmetric pullout load spectrum (9 at the 124 knot airspeed and 4 at the 155 knot airspeed) and the two model 95 percentile load spectrums. The different interval sizings provided slightly different damage calculations. The interval sizing taken directly from Sikorsky's substantiation runs proved to be the most conservative and thus was the interval set used for comparisons for damage calculations. The damage calculated for the 155 knot, 16,500 lbs. gross weight, model run was 3.7542 x 10E-4. The damage calculated for Sikorsky's, 155 knot, 19,000-21,000 lbs. gross weight, substantiation run was 1.0 x 10E-4. See Table 3 for a summary of the 155 knot runs damage calculations.

TABLE 3: DAMAGE CALCULATED FOR 155 KNOT RUNS
20 OCCURRENCES

RUN	DAMAGE CALCULATED INTERVAL 1 BIN SIZE	DAMAGE CALCULATED INTERVAL 2 BIN SIZE	DAMAGE CALCULATED W/ MEAN LOAD CORRECTION
MODEL 155 KNOT RUN	3.073E-4	3.753E-4	N/A
RUN 28	3.698E-5	5.393E-5	4.000E-7
RUN 29	3.501E-4	3.960E-4	1.190E-5
RUN 30	1.115E-4	1.618E-4	2.460E-6
RUN 31	4.335E-4	4.624E-4	3.586E-5
SUBSTANTIA TION RUN (FIGURE 1)	N/A	1.000E-4	N/A

The damage calculated for the individual runs varied from the model run by 10 times less to 1.25 times more. The model runs seemed to compare well with the individual runs in the fatigue analysis. The damage calculated for the model run was 3.5 - 4.0 times more than the substantiation run. This comparison indicated that the model run was more conservative than the substantiation run in the fatigue analysis.

E. MEAN LOAD INFLUENCES

The mean load influences the damage calculated on a component. For a given maximum load spectrum, one which oscillates around a zero mean load will cause more damage than

one which oscillates around a load greater than zero. In this study, the component S-N curve incorporated a mean load of 2200 lbs. If the mean of the oscillating load were larger than 2200 lbs., the resulting damage would be reduced.

1. **Rainflow Counting**

To determine the mean load for each cycle, the rainflow counting method was used. It counted the cycles in the load-time history [Ref. 12]. This method determined the range between upper and lower bounds, as well as the mean load for each load reversal. (See Appendix C for a description of the Rainflow Counting Method [Ref. 13].)

2. **Goodman Correction**

The method used by Sikorsky did not adjust the oscillatory loads by their true mean load level. Instead, an average mean level correction of 2200 lbs was incorporated into the component S-N curve. To calculate the effects of the true mean load level on each maximum load in the fatigue analysis, each maximum load component S-N curve was modified by a Goodman correction. See Appendix C, for the Goodman correction equation. The resulting Goodman equation, used to shift the component S-N curve, was based on the Haigh diagram for a line of constant life of 10E8. See Figure 28 for a description of the Haigh diagram.

59
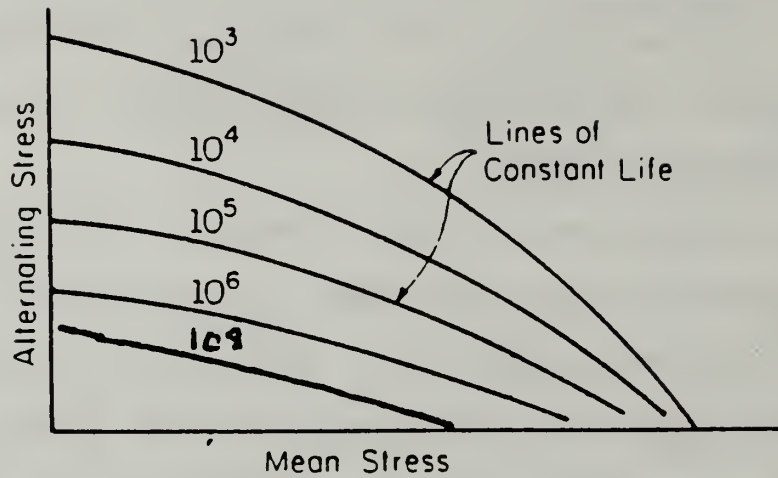
Figure 28: Haigh Diagram

The mean load correction equation is given in Equation (13).

$$\frac{S_{max\infty} - S_{mean}}{S_{max0}} + \frac{S_{mean}}{S_{ultimate}} = 1 \qquad (13)$$

Where $S_{max\ 0}$ represents the endurance load at zero mean load and all terms are given in lbs. The ultimate load was calculated from the ultimate stress using a bearing stress equation, Equation (14). This equation determined the average nominal value of the ultimate bearing stress [Ref. 14].

$$\sigma = \frac{P}{d\,t} \qquad\qquad (14)$$

Where P = $S_{ultimate}$ and $\sigma = \sigma_{ultimate}$. The ultimate stress, $\sigma_{ultimate}$, for 7075-T73 aluminum was 69,000 psi. The diameter (d) of the bearing was .75 inch and the thickness (t) was 1 inch. The load was then reduced by four as there were four servo beam rails per servo. The ultimate load, $S_{ultimate}$, with no alternating loads applied, was 12,938 lbs.

To find $S_{max\ 0}$, Equation (15) was used with the test condition of the component S-N curve; S_{mean} = 2200 lbs. and $S_{max\ infinity}$ = 5211 lbs. as calculated from Equation (11). Using the experimental endurance limit value of 4871 lbs., the resulting value for $S_{max\ 0}$ was 3627 lbs. Equation (15) becomes:

$$\frac{S_{max\ \infty} - S_{mean}}{3627} + \frac{S_{mean}}{12,938} = 1 \qquad\qquad (15)$$

For a given cycle, S_{mean} and S_{max} were determined. Using S_{mean}, an equivalent endurance limit, $S_{max\ infinity}$, can be calculated from equation (15) and inserted into the expression for the new component S-N curve, Equation (11). The resulting equation is Equation (16).

$$S_{max} = (.61) S_{max\infty} (1 + . \frac{483}{\sqrt{N}}) \tag{16}$$

The S_{max} for the cycle can then be used to calculate the number of cycles to failure at that level N. With N, the damage can be calculated for that cycle using Equation (12).

3. Comparison with Component S-N Results

Correcting for the mean load reduced the resulting load seen by the component. The amount of damage this load caused reduced the damage calculated by approximately 10 to 100 times. See Table 3 for a comparison of damage calculations with and without the mean load correction.

V. SUMMARY AND CONCLUSIONS

A. SUMMARY

The safe life fatigue analysis method is used by the Navy to determine the life of critical helicopter components. The servo beam rail of the SH-60B helicopter was the critical component studied in this report. Historically, the safe life method employed many assumptions which were believed to increase the conservatism of the analysis; thus, increasing the reliability. The flight loads on the component were identified as a dominant factor in the determination of a safe life analysis. Statistical methods were used to understand the distribution of this factor. The distribution of loads in the symmetric pullout maneuver were studied and found to represent two populations of loads, upper and lower. The upper population was researched further and found to have sub-populations depending on the gross weight, the flight speed, and the collective setting. The gross weight sub-population was evident when looking at the maximum load data. When the gross weight was increased the maximum load on the component increased. The airspeed sub-population was evident when comparing the upper loads of the individual symmetric pullout runs. The higher the airspeed the higher the number of upper loads. Due to unavailability of data, sub-populations developed due to differences in collective setting could not

be explored. There was evidence that the top collective position greatly increased the upper loads compared to the -25 percent collective setting and the fixed collective setting.

With these sub-populations identified, attempts to statistically model the distributions were made. The Weibull distribution was used to model the loads from the sub-population of the individual symmetric pullout maneuvers. The model was successful in representing the two sub-populations of data at 124 knots and 155 knots. However, more data would have been highly desirable to give full confidence in its reliability. .

The extreme value distribution modeled the maximum loads in order to understand the upper load percentiles. The upper load percentiles were needed to understand the level of conservatism used in the current safe life fatigue analysis which used the Sikorsky substantiation run for the servo beam rail component. The substantiation run was expected to be at the 50th percentile or higher as it was the highest load run out of four or five substantiation runs. The maximum load of the 55 knot, 2.5 "g" load and higher, substantiation run was at approximately the 45th percentile of lower gross weight extreme value model and the 20th percentile of the combined gross weight extreme value model.

Fatigue life calculations were completed for 13 runs of the original load spectrum (9 at the 124 knot airspeed and 4 at the 155 knot airspeed) and the two model, 95 percentile load spectrums (See Figure 18 and 19). Two load interval sizing schemes were used in the fatigue calculations. The load interval sizing taken directly from Sikorsky's fatigue analysis of this component proved to be the most conservative and thus was used as the comparative interval for damage calculations. The model runs seemed to indicate a good representation of the individual runs when comparing the fatigue analysis. The damage calculated for the model 124 knot run was 4.211 x 10E-5, while the damage calculated for the 9 individual runs ranged from 0 to 4.318 x 10E-5 damage. An increase in "g" loading represented an increase in component damage. The damage calculated for the model 155 knot run was 3.7542 x 10E-4, while the damage calculated for the four individual runs ranged from 5.393 x 10E-5 to 4.6237 x 10E-4. The model run was compared to the Sikorsky substantiation run at 155 knot airspeed and over 2.5 "g" load. The damage for the Sikorsky run was 1.0 x 10E-4. This indicated that the Sikorsky substantiation run was less conservative.

Corrections were made to take into consideration in the damage calculation the change in the mean load for each maximum load level. These corrections lowered the resulting

effective load so that less damage was accrued by the component during the maneuver.

B. CONCLUSIONS

Statistical analysis can be used to describe the random load spectra for symmetric pullout maneuvers for use in safe life fatigue analyses. These models provide an understanding of the level of conservatism of the current fatigue methods. More data could be searched to build greater confidence in the reliability of these models.

Several variables affect the statistical analysis by creating sub-populations in the data. Velocity and gross weight formed two obvious sub-populations. The results determined from the statistical analysis were not always as expected. Specifically, the maximum load percentile for the substantiation run was lower than the 50th percentile of the extreme value model for the same airspeed and gross weight.

Taking into account the mean load, reduced the damage calculated for the critical component by a factor of 10 to 100. This reduction indicated that the whole method might be overly conservative. With this large influence from the mean loads, more research is warranted to back up these findings.

REFERENCES

1.   Schneider G. and Gunsallus C., "Continuation of the AHS Round Robin on Fatigue Reliability and Damage Tolerance".

2.   Zion, H. Lewis, "Safe Life Reliability: Evaluation of New Statistical Method", American Helicopter Society Annual Forum, Phoenix, Arizona, May 1991.

3.   Viswanathan, S.P., Tata, V., Boorla, R., Mcleod, G., and Slack, J., "A Statistical Analysis to Assess the Reliability of a Rotor-craft Component in Fatigue", 43rd Annual National Forum of the American Helicopter Society, St. Louis, Missouri, May 1987.

4.   United Technologies, Sikorsky Aircraft, "Methods of Structural Reliability Substantiation of Navy H-60 Components Based on Laboratory Fatigue and Flight Test Data, SER-520103, 1986.

5.   Edwards, P.r. and Darts, J., "Standardized Fatigue Loading Sequences for Helicopter Rotors (Helix and Felix), Parts 1 and 2, Reports Nos. TR84084 and TR84085, Royal Aircraft Establishment, Ministry of Defense, England, 1984

6.   Dowling, Norman E., Krasnowski, Boydon R., Viswanathan, Sathy P., "Design, Analysis and Testing Considerations of Fatigue Critical Rotorcraft Components", National Technical Specialist Meeting of the American helicopter Society on Advance Rotocraft Structures, Virginia, 1988.

7.   Khosrovanch, A.K., Dowling, N.E., Berens, A.P., and Gallagher, J.P., "Fatigue Life Estimates for Helicopter Loading Spectra", U.S. Army Aviation Applied Technology Directorate, Fort Eustis, Virginia.

8.   NATOPS Flight Manual, Navy Model SH-60B Aircraft, Chief of Naval Operations, 15 June 1990.

9.   Cox, D.R., and Oakes, D., "Analysis of Survival Data", Chapman & Hall, London, 1985.

10.   Bury, Karl V., "Statistical Models in Applied Science", John Wiley & Sons, New York, 1987.

11.   Barndt, Gene, NAVAIR, Aerospace Engineer, "Personal Correspondence by Facsimile", 1450, 28 April 1992.

12.   Bannantine, Julia A., Ph.D., Cromer, Jesse J., Ph.D., Hardrock, James L., Ph.D., "Fundamentals of Metal Fatigue Analysis, Prentice Hall, 1990.

13. "Standard Practice for Cycle Counting in Fatigue Analysis", 1986, Annual Book of ASTM Standards, Bol. 03.01, Standard No. E1049.

14.   Beer, Ferdinand P., Johnston, E. Russel, Jr., "Mechanics of Materials", Mcgraw-Hill Book Company, New York, 1981.

15.   Johnson, Norma J., "Continuous Univariate Distributions-1", John Wiley & Sons, Inc., Salt Lake City, Utah, 1970.

16.   Wadsworth, Harrison M., "Handbook of Statistical Methods for Engineers & Scientist", Mcgraw-Hill Publishing, New York, 1990.

17.   Lewis, E.E., "Introduction to Reliability Engineering:, John Wiley & Sons, Inc., New York, 1987.

18.   D'Agostino, Ralph B, and Stephens, Michael A., "Goodness of Fit Techniques", Marcel Dekker, Inc., New York, 1986.

APPENDIX A: REVIEW OF STATISTICAL MODELS

This appendix briefly discusses probability distributions and their use in summarizing, interpreting, and analyzing data. It specifically looks at six distributions. An understanding of the physical characteristics of the data is important in distribution selection. Yet, without a clear understanding of the physical characteristics the choice of distribution can still be determined. In these instances the distribution simply becomes a mathematical model for the data.

The **normal distribution** is the most frequently used distribution and is quite often a good model for the distribution of variables representing many natural phenomena which may be expected to be reasonably symmetric [Ref. 15]. It gives the best representation when the mean area is of importance. The Central Limit Theorem states that the normal distribution is appropriate when the measurement is produced by the sum of many random variables, or in other words the observation arises from the cumulative effect of a large number of factors [Ref. 16]. The two parameters which describe this function are the mean and the standard deviation. See Table A-1 for the density (pdf) and cumulative density function (cdf) equations.

The **Weibull distribution** is the most universally employed distribution when modeling aging effects as a time-to-failure model since by proper choice of its parameters it can represent the lifetime characteristics of a wide diversity of equipment. Its two parameters are shape and scale. The value of the shape parameter indicates the versatility of the Weibull distribution. When the shape function is greater than 1.0 the failure rates are typical of aging effects, the component gets worse with time. When the shape parameter equals 3.44 the normal distribution is approximated and when it equals 1.0 the Weibull distribution corresponds to the exponential distribution. [Ref. 16] The scaling parameter determines the spread of the values. The estimation of the parameters can be difficult. The maximum-likelihood technique, which requires the solution of two nonlinear equations, is typically used. See Table A-1 for the density (pdf) and cumulative distribution function (cdf) equations.

The **gamma distribution** is used to represent the failure of some mechanism where failure is caused by an accumulation of damage. It is derived as the distribution of the sum of independent, identically distributed exponential random variables. The two parameters are the shape and scale. When the shape is less that 1.0 the conditional failure rate decreases to the lower bound. When the shape equals 1.0 the exponential model is obtained with a constant failure rate.

70

When the shape parameter is greater than 1.0 the conditional failure rate increases to an upper bound. As the shape gets larger it approaches the normal distribution [Ref. 15]. See Table A-1 for the density (pdf) and cumulative distribution function (cdf) equations.

The **lognormal distribution** is useful when the uncertainty about the load, or capacity, or both is relatively large [Ref. 17]. It can be derived as the appropriate lifetime model where failure of a unit occurs only when damage to it has reached a specific level. It is similar to the normal distribution except that instead of the random variable X being summed by the individual random variables (x's) the random variable Y is the product of the individual random variables (y's). For example, the wear on a system may be proportional to the product of the magnitudes of the demands that have been made on it [Ref. 17]. Thus, if the phenomena is the product of many factors the lognormal may be appropriate. Both the normal and lognormal distribution are useful in representing the upper tail of the load distribution when there are many contributions no one of which is dominant. The two parameters which describe the lognormal distribution are the log mean and the log standard deviation. See Table A-1 for the density (pdf) and cumulative distribution function (cdf) equations.

71

The **extreme value distribution** is used when the random variable of interest represents the occurrence of an extreme. It is needed when the upper tail of the load distribution is not determined by either the sum or the product of many relatively small contributions [Ref. 15] but by the extreme of the many contributions which governs the load or the capacity. For example, it is not the sum of the flaw contributions, but rather the extreme value that may limit the capacity of a pressure vessel [Ref. 16]. Its two parameters are the location and scale parameter. The location is the mode of the distribution. See Table A-1 for the density (pdf) and cumulative distribution function (cdf) equations.

The **exponential distribution** is used as a constant failure rate model for continuously operating systems. It has the property of "memorylessness" [Ref. 16]. Thus, the probability of failure within a specified time interval is independent of the age of the component. Physically this would be used when the random failures are caused by external shocks and they are not dependent on the components past history.

TABLE A.1: DISTRIBUTION PDF AND CDF EQUATIONS

Distribution Table		
Normal	pdf	$f(x) = \dfrac{1}{\sqrt{2\pi}\sigma} \exp \dfrac{-(x-\mu)^2}{2\sigma^2}$
	CDF	$F(x) = \int_{-\infty}^{\infty} \dfrac{1}{\sqrt{2\pi}\sigma} \exp -\dfrac{(x-\mu)^2}{2\sigma^2}$
Wei-bull	pdf	$f(x) = \alpha\beta(x)^{\beta-1} \exp(-\alpha x^\beta)$
	CDF	$F(x) = 1 - \exp(-(\alpha x)^\beta)$
Gamma	pdf	$f(x) = \dfrac{\beta}{\Gamma(\alpha)} x^{\alpha-1} x (-\beta x)$
Expo-nen-tial	pdf	$f(x) = \lambda \exp(-\lambda x)$
	CDF	$F(x) = 1 - \exp(-\lambda x)$
Log-normal	pdf	$f(v) = \dfrac{1}{\sqrt{2\pi}\sigma x} \exp\left\{ -\dfrac{1}{2}\left[\dfrac{\ln x - \mu}{\sigma} \right]^2 \right\}$
Ext-reme Value	pdf	$f(x) = \dfrac{1}{\alpha} \exp\left(-\dfrac{1}{\alpha}(x-\mu) - \exp\left(-\dfrac{1}{\alpha}(x-\mu)\right)\right)$
	CDF	$F(x) = \exp\left(-\exp\left(\dfrac{1}{\alpha}(x-\mu)\right)\right)$

APPENDIX B: GOODNESS-OF-FIT TESTS

This appendix looks at the goodness of fit tests based on the empirical cumulative distribution function (ECDF). The ECDF is the step function, calculated from the sample, which estimates the population distribution function. The ECDF statistics measure the discrepancy between the ECDF, $Fn(x)$, and a given distribution function, $F(x)$. D'Agostino and Stephens provided the background for this Appendix. [Ref. 18] Goodness-of-fit techniques were used for this study as the parameters for the distribution were unknown. The method of calculating the goodness-of-fit statistic involved: 1) stating the hypothesis (the hypothesis for this study stated that the sample could be modeled by a certain distribution), 2) calculating the statistic using the given equation, 3) Comparing the statistic value to the upper tail levels of significance. If the statistic exceeded the upper tail value, the hypothesis was rejected. Every statistic was married with a P-value. If the P-value was less than .15 the hypothesis was rejected. In other words, for a good fit, the smaller the statistic, the better the fit, and the larger the P-value, the better the fit.

For case three fitting the parameter or parameters to the same sample from which the goodness-of-fit tests were determined, made it possible to adjust the tested distribution

to the sample in such a way that the statistic can detect a departure from the original distribution with roughly the same efficiency as if the parameters were previously known. The Anderson-Darling (A^2) statistic appears to be the most effective at detecting departure in the tails. The superiority of the Anderson-Darling statistic was also documented by various power studies. [Ref. 18]

The Anderson-Darling statistic is a weighted Cramer-von Mises statistic [Ref. 18]. The percentage points for finite sample sizes converge rapidly to the percentage points of the asymptotic distribution of the Anderson-Darling statistic.

APPENDIX C: RAINFLOW COUNTING METHOD

This appendix briefly discusses the rainflow counting method, which is a procedure for interpreting irregular load versus time history as a collection of events (called cycles) to which fatigue damage can be assigned. It is a cycle counting method which attempts to identify closed hysteresis loops in the stress-strain response of a material subjected to cyclic loading [Ref. 12]. In this method cycles are counted depending on the comparison of two adjacent ranges. If the first range is less than or equal to the second, a cycle is counted and the corresponding peak and valley are discarded for purposes of further cycle counting. [Ref. 13]

The rules for rainflow counting are as follows [Ref. 13]:

1) Let X denote range under consideration; Y, previous range adjacent to X; Arrange history to start with either the maximum peak or minimum valley.

2) Read the next peak or valley. If out of data stop.

3) If there are less than 3 point, go to Step 2. Form ranges X and Y using the three most recent peaks and valleys that have not been discarded.

4) Compare the absolute value of range X and Y.
   a) If X < Y go to Step 2.
   b) If X > or = Y go to Step 5.

5) Count range Y as one cycle; discard the peak and valley of Y; go to Step 3.

Figure C.1 depicts an example of a strain time history and how using rainflow counting the hysteresis loops are determined. Four of the events resemble constant amplitude

76

behavior: A-D, B-C, E-F, G-H. These events occur as closed
hysteresis loops, each having its own strain range and mean
stress/load values. To calculate the damage, the hysteresis
loops are counted and the fatigue life is calculated using two
methods. The first method is the strain-life equation which
incorporates the mean stress/load effects. The second method
is the component S-N curve. This method assumes that the mean
stress/load of the component S-N curve accounts for the mean
stress/load seen by the vibratory stress/load. If the mean
stress/load is less than the vibratory mean stress/load a
correction is made. The mean stress/load correction equations
are used, such as the Soderberg, the Goodman, the Gerber, or
the Morrow [Ref. 12]. Equation C.1 is the Goodman equation.
These two methods will provide the life to failure and from
that using Minor's linear damage rule the damage is
calculated.

$$C.1) \quad \frac{\sigma_a}{S_e} + \frac{\sigma_m}{S_u} = 1$$
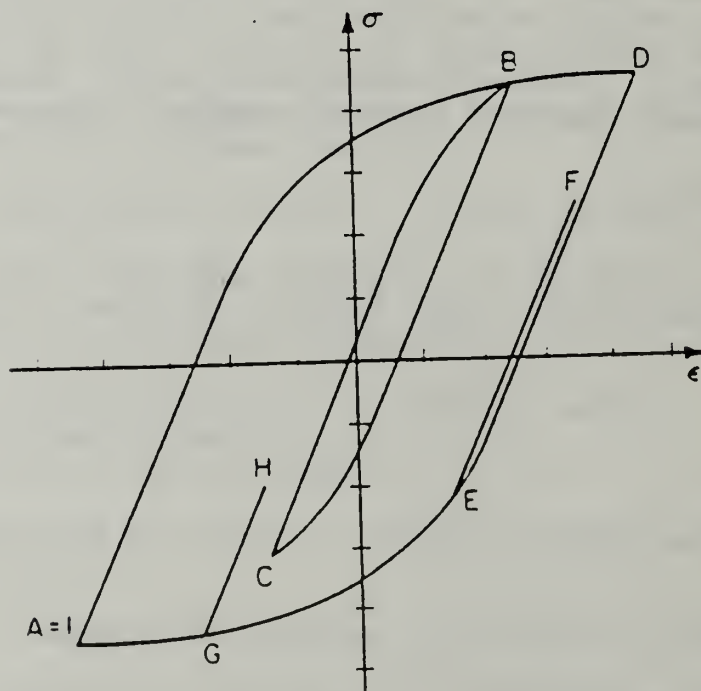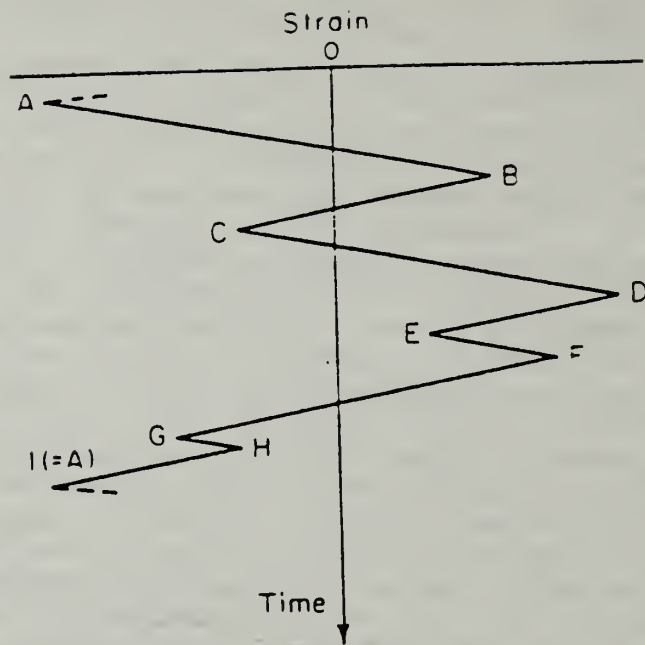
Figure C.1: Material Stress-Strain Response to Strain History

INITIAL DISTRIBUTION LIST

1. Defense Technical Information Center   2
    Cameron Station
    Alexandria, Virginia   22304-6145

2. Library, Code 0142   2
    Naval Postgraduate School
    Monterey, California   93943-5002

3. Chairman   1
    Department of Aeronautics, Code AA
    Naval Post Graduate School
    Monterey, California   93943

4. Ms. Robin Imber   1
    Systems Engineering Division, Code 1260
    David Taylor Research Center
    Carderockdiv Laboratory
    Bethesda, Maryland   20084-5000

5. Professor Gerald H. Lindsey   1
    Department of Aeronautics, Code AA/LI
    Naval Post Graduate School
    Monterey, California   93943

6. Lieutenant Sally deGozzaldi, USN   1
    147 Belknap Road
    Framingham, Massachusetts   01701